urea nitrogen (BUN), creatinine, glucose, total cholesterol, triglycerides, phospholipid, Na, K, Cl, Ca, inorganic phosphate, aspartate aminotransferase (AST), alanine aminotransferase (ALT), lactase dehydrogenase (LDH), and gamma-glutamyltransferase (γ-GTP).

In the main group, daily vaginal lavage samples of each female were evaluated for estrous cyclicity throughout the premating period. Each female rat was mated overnight with a single male rat of the same dosage group until copulation occurred or the 2-week mating period had elapsed. During the mating period, daily vaginal smears were examined for the presence of sperm. The presence of sperm in the vaginal smear and/or a vaginal plug was considered as evidence of successful mating. Once insemination was confirmed, the females were checked twice a day for signs of parturition from day 21 to day 24 of pregnancy. One female in the 0.1 mg/kg/day treatment group did not deliver and did not have implantation. Because of infertility, data for that female for the period corresponding to gestation were excluded from statistical analysis. Other females were allowed to deliver spontaneously and nurse their pups until postnatal day (PND) 4. The day on which parturition was completed by 17:00 was designated as PND 0. Litter size and numbers of live and dead pups were recorded, and live pups were sexed and individually weighed on PNDs 0 and 4. Pups were inspected for external malformations on PND 0. On PND 4, the pups were euthanized by exsanguination under anesthesia, and gross internal examinations were performed.

Data analysis

Statistical analysis of pups was carried out using the litter as the experimental unit. Mean and standard deviation in each dose group were calculated for body weight, food consumption, water consumption, number of feces, rearing frequency, width of the landing legs, grip strength, spontaneous motor activity, urine volume, hematological test results, blood biochemical test results, absolute and relative organ weights, estrous cycle length, length of gestation, numbers of corpora lutea and implantations, implantation index, total number of pups born, number of male and female pups, number of live and dead pups, live birth index, live pups and viability index on day 4 of lactation, and body weight of pups. These were analyzed with Bartlett's test or F-test for homogeneity of variance. If they were homogeneous, the data were analyzed using Dunnett's test or Student's t-test to compare the mean of the control group with that of each dosage group, and if they were not homogeneous, a Dunnett-type rank test or Aspin-Welch t-test was applied. The copulation index, fertility index, gestation index, sex ratio of pups, and data for sensory reactions of reflexes were analyzed with Yates' chi-square test. The 5% levels of probability were used as the criterion for significance. Unless otherwise noted, there are statistically significant differences in the changes described in the following Results section.

RESULTS

Parental toxicity

No deaths were observed in any of the groups. A decrease in grip strength of the forefoot was observed in males and females at 1.0 mg/kg/day in the recovery period. No other treatment-related effects on clinical signs of toxicity, FOB, sensory reactivity, or spontaneous motor activity were observed in males and females in the main and satellite groups (data not shown).

Body weight changes in each group are shown in Figs. 1 and 2. In males at 1.0 mg/kg/day, body weight gains decreased during the dosing period and during the recovery period. In females at 1.0 mg/kg/day, body weight gains decreased during the lactation period in the main group and during the dosing period and the recovery period in the satellite group, and lowered body weight was observed on days 38 and 41 of the dosing period and on days 0-13 of the recovery period in the satellite group. No effects on body weight in male and female groups were observed at any other dosing. Food consumption (data not shown) was decreased on day 4 of the delivery period at 1.0 mg/kg/day in females. Urinalysis revealed no significant differences in any parameters between the control and treatment groups in males and females in the main and satellite groups (data not shown).

Table 1 shows hematological findings in male and female rats. At 1.0 mg/kg/day, low values of fibrinogen and APTT were observed in males of the main and satellite groups, and a low value of fibrinogen was observed in females of the main group. The other significant changes in hematological findings were incidental because they were slight without related changes or did not occur in a dose-dependent manner.

Blood biochemical findings are shown in Table 2. At 1.0 mg/kg/day in the main group, increases in BUN and ALP and decreases in total protein and albumin were observed in males, and an increase in BUN and a decrease in total protein were observed in females. At 1.0 mg/kg/day in the satellite group, increases in BUN and ALP in males and females, and a decrease in total protein in females were observed. The other changes with statistical significances in blood biochemical findings were incidental because they were slight without related changes or did not occur in a dose-dependent manner.

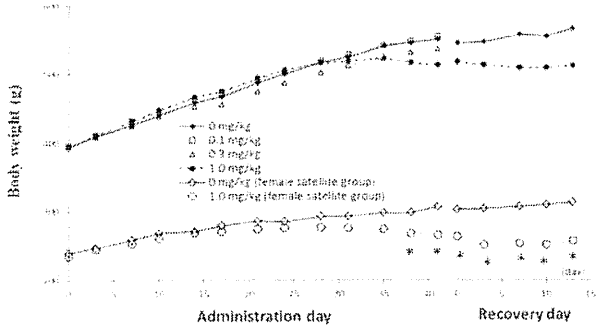

Fig. 1. Body weight of males in main groups and satellite groups for recovery period and females in satellite groups.
*: Significantly different from the control, $p \leqq 0.05$.

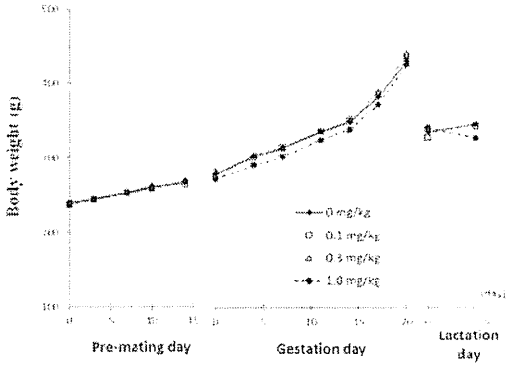

Fig. 2. Body weight of females in main groups.

Organ weights in males and females are shown in Table 3. Relative weight of the liver was increased at 0.3 mg/kg/day in main group males, and absolute and relative weights of the liver were increased in males and females at 1.0 mg/kg/day in main and satellite groups. Absolute and relative weights of the spleen were decreased at 1.0 mg/kg/day in main group males. Enlargement of the liver in two males and a dark red focus in the stomach in three males were observed at 1.0 mg/kg/day in the main group. No other treatment-related findings at necropsy were observed in males and females in main and satellite groups. Histopathological findings are shown in Table 4. Possibly treatment-related changes were observed in the liver and stomach: In the main groups, centrilobular hypertrophy of hepatocytes in males and females were observed at 0.3 mg/kg/day and above, diffuse vacuolation of hepatocytes in males, and minimal focal necrosis in males and females were observed at 1.0 mg/kg/day, and in the satellite groups, minimal diffuse vacuolation of hepatocytes in males, centrilobular hypertrophy/degeneration of hepatocytes in males and females, and Glisson's sheath cell infiltration in females were observed at 1.0 mg/kg/day. In the glandular stomach, minimal erosion was observed in 3/7 males at 1.0 mg/kg/day. Although a similar change was observed in 2/6 control females, the possibility that PFUA treatment affected the stomach in males could not be ruled out. The findings in other organs were considered to be incidental in main and satellite groups, because there was no dose-dependent increase in incidence or severity. On reproductive organs, no treatment-related histopathological changes were found in the epididymides, testis, and uterus in PFUA-treated groups.

Reproductive and developmental findings

There were no significant differences in the mean estrous cycle and in the incidence of females with a normal estrous cycle between the control and PFUA groups either in the main or recovery group (data not shown). The data for reproductive and developmental parameters are shown in Table 5. Reproduction performance of parental rats, delivery and nursing were not significantly different between the control and PFUA-treated groups. Regarding the general appearance of pups, there were no abnormal findings in any groups. The body weights of male and female pups on PNDs 0 and 4 were lowered at 1.0 mg/kg/day. There were no significant differences in the sex ratio of live pups or the viability index on PND 4. At gross pathology in pups on PND 4, thymic remnant in the neck was observed in one male and one female at 0.3 mg/kg/day, and in two females at 1.0 mg/kg/day, and these were considered to be incidental because of the low incidence. There were no other changes in gross internal findings of pups in any PFUA-treated groups.

DISCUSSION

The present study of rats was conducted to examine the possible effects of PFUA on reproduction and development as well as the possible general toxic effects. The dosage of PFUA used in this study was sufficiently high to be expected to induce general toxic effects in parental animals. The following results suggest that the liver is a sensitive target organ. The weight of the liver was increased in males at 0.3 mg/kg/day and above, and in females at 1.0 mg/kg/day, and centrilobular hypertrophy of hepatocytes was observed in both sexes at 0.3 mg/kg/day and above, focal necrosis and/or diffuse vacuolation of hepatocytes were also found in the 1.0

Table 1. Hematological findings

		Main group				Satellite group	
	Group	0 mg/kg/day	0.1 mg/kg/day	0.3 mg/kg/day	1.0 mg/kg/day	0 mg/kg/day	1.0 mg/kg/day
Males							
Number of animals		5	5	5	5	5	5
WBC	(10^2/μl)	121.2 ± 31.4	94.8 ± 21.1	127.6 ± 35.4	129.8 ± 23.5	73.4 ± 26.8	111.6 ± 19.5*
RBC	(10^4/μl)	830 ± 40	846 ± 25	852 ± 20	869 ± 23	894 ± 34	886 ± 47
HGB	(g/dl)	15.6 ± 0.4	15.7 ± 0.6	15.4 ± 0.4	15.6 ± 0.7	16.0 ± 0.4	15.3 ± 0.9
MCV	fl	52.5 ± 1.8	51.4 ± 1.7	50.6 ± 0.7	50.1 ± 1.4*	50.9 ± 1.5	49.4 ± 1.9
MCH	pg	18.8 ± 0.5	18.6 ± 0.8	18.1 ± 0.4	17.9 ± 0.4*	17.9 ± 0.3	17.3 ± 0.7
Platelet	(10^4/μl)	98.7 ± 3.7	121.4 ± 5.2**	109.2 ± 8.8	111.2 ± 8.8*	107.8 ± 12.4	122.7 ± 18.6
APTT	(sec)	22 ± 4.1	19.2 ± 1.9	20.8 ± 4.2	16.6 ± 0.7*	20.4 ± 1.7	17.2 ± 2.6*
Fibrinogen	mg/dl	294 ± 20	273 ± 35	283 ± 31	200 ± 23**	304 ± 35	245 ± 22*
Females							
Number of animals		5	5	5	5	5	5
WBC	(10^2/μl)	143.4 ± 43.8	128.7 ± 25.4	151.8 ± 33.5	159.2 ± 45.1	58.6 ± 14.9	65.1 ± 13.6
RBC	(10^4/μl)	702 ± 46	680 ± 67	692 ± 50	645 ± 51	830 ± 30	846 ± 56
HGB	(g/dl)	13.1 ± 1.0	13.5 ± 1.0	13.5 ± 1.1	13.2 ± 0.8	15.4 ± 0.4	15.4 ± 1.0
MCV	fl	52.7 ± 1.3	56.7 ± 4.5	55.0 ± 1.2	58.0 ± 3.1*	51.4 ± 1.4	50.1 ± 1.2
MCH	pg	18.6 ± 0.5	20.0 ± 1.6	19.5 ± 0.6	20.5 ± 1.1*	18.6 ± 0.6	18.2 ± 0.6
Platelet	(10^4/μl)	159.4 ± 27.4	141.0 ± 22.7	164.8 ± 19.6	161.8 ± 30.9	130.6 ± 13.7	125.7 ± 18.1
APTT	(sec)	17.6 ± 1.8	17.5 ± 2.4	17.9 ± 2.3	15.2 ± 3.3	17.9 ± 2.3	17 ± 2.9
Fibrinogen	mg/dl	335 ± 53	319 ± 95	282 ± 49	228 ± 42*	207 ± 10	176 ± 31

Values are given as the mean ± S.D.
*: Significantly different from the control, $p \leqq 0.05$. **: Significantly different from the control, $p \leqq 0.01$.

mg/kg/day group. In rodents, it is clear that the hepatic response to exposure to many perfluoroalkyl compounds is initiated by the activation of the nuclear hormone receptor, PPARα (ATSDR, 2009), and PFUA activates mouse PPARα *in vitro* (Wolf *et al.*, 2012). The hepatic proliferative responses, including an increase in the liver weight and centrilobular hypertrophy of hepatocytes, observed in the present study might have been initiated by the activation of PPARα, although there is a scientific consensus that compounds which are peroxisome proliferators in rodents have little or no effect on human liver (IARC, 1995). Regarding the toxicity of PFAAs, the involvement of mechanisms other than PPARα has been suggested (Peters and Gonzalez, 2011), so further research on the toxicity mechanism of PFUA is desired.

Effects on the body weight of adult males/females and pups were observed only at 1.0 mg/kg/day. In adult animals, suppression of body weight gain was observed in males/females in the administration and/or recovery periods, although not in females in the premating and gestation periods. It is considered that these body weight changes were a direct effect of PFUA because they were not related to food consumption. There is a possibility of maternal-fetal/infant transfer of PFUA, because maternal-fetal transfer and maternal-infant transfer of PFOA through breast milk have been observed in rats (Hinderliter *et al.*, 2005). Because there was no difference in the length of the gestation period in dams dosed at 1.0 mg/kg/day compared to the controls, and because sup-

Table 2. Blood biochemical findings

		Main group				Satellite group	
	Group	0 mg/kg /day	0.1 mg/kg/day	0.3 mg/kg/day	1.0 mg/kg/day	0 mg/kg/day	1.0 mg/kg/day
Males							
Number of animals		5	5	5	5	5	5
AST	(IU/l)	67 ± 9	70 ± 4	73 ± 17	77 ± 6	62 ± 9	73 ± 12
ALT	(IU/l)	31 ± 3	32 ± 3	34 ± 3	39 ± 7*	31 ± 5	37 ± 5
ALP	(IU/l)	427 ± 12.6	461 ± 85	514 ± 96	1021 ± 179**	379 ± 95	707 ± 152**
Total cholesterol	(mg/dl)	56 ± 14	47 ± 8	34 ± 6**	46 ± 11	55 ± 18	53 ± 13
Triglyceride	(mg/dl)	48 ± 10	70 ± 42	41 ± 9	46 ± 16	52 ± 17	45 ± 27
Phospholipid	(mg/dl)	90 ± 13	82 ± 14	65 ± 9*	87 ± 11	87 ± 19	92 ± 21
BUN	(mg/dl)	13 ± 2	14 ± 3	15 ± 1	21 ± 4**	17 ± 2	23 ± 5*
Na	(mmol/l)	147 ± 2	146 ± 2	147 ± 1	145 ± 1	145 ± 1	143 ± 1**
Cl	(mmol/l)	108 ± 2	108 ± 1	109 ± 1	109 ± 3	107 ± 1	108 ± 1
Ca	(mg/dl)	10.1 ± 0.2	10.0 ± 0.3	10.0 ± 0.3	9.7 ± 0.2*	9.9 ± 0.3	9.5 ± 0.3
Total protein	(g/dl)	6.2 ± 0.2	6.0 ± 0.3	6.1 ± 0.1	5.5 ± 0.3**	6.3 ± 0.1	5.8 ± 0.5
Albumin	(g/dl)	2.8 ± 0.1	2.8 ± 0.1	2.9 ± 0.0	2.6 ± 0.1*	2.7 ± 0.1	2.8 ± 0.2
A/G		0.80 ± 0.07	0.86 ± 0.03	0.93 ± 0.05**	0.88 ± 0.06	0.77 ± 0.04	0.93 ± 0.09**
Females							
Number of animals		5	5	5	5	5	5
AST	(IU/l)	84 ± 21	92 ± 12	86 ± 15	81 ± 12	59 ± 4	68 ± 11
ALT	(IU/l)	53 ± 9	55 ± 12	50 ± 18	49 ± 1	26 ± 4	28 ± 4
ALP	(IU/l)	219 ± 72	242 ± 42	286 ± 176	263 ± 18	158 ± 28	289 ± 54**
Total cholesterol	(mg/dl)	60 ± 11	52 ± 13	41 ± 13*	49 ± 8	78 ± 16	64 ± 14
Triglyceride	(mg/dl)	54 ± 11	38 ± 12	41 ± 18	60 ± 25	28 ± 11	20 ± 3
Phospholipid	(mg/dl)	112 ± 13	94 ± 18	80 ± 20*	98 ± 11	141 ± 20	108 ± 15*
BUN	(mg/dl)	13 ± 2	13 ± 4	16 ± 3	19 ± 2**	20 ± 3	29 ± 7*
Na	(mmol/l)	141 ± 1	141 ± 2	143 ± 1	142 ± 1	143 ± 1	143 ± 1
Cl	(mmol/l)	106 ± 1	107 ± 2	108 ± 2	108 ± 2*	109 ± 1	112 ± 2
Ca	(mg/dl)	10.3 ± 0.2	10.2 ± 0.4	10.3 ± 0.1	10.0 ± 0.3	10.2 ± 0.3	9.9 ± 0.2
Total protein	(g/dl)	6.2 ± 0.2	5.8 ± 0.3*	6.0 ± 0.1	5.6 ± 0.2**	6.7 ± 0.2	5.8 ± 0.3**
Albumin	(g/dl)	2.8 ± 0.2	2.8 ± 0.2	2.8 ± 0.1	2.7 ± 0.2	3.1 ± 0.2	2.9 ± 0.3
A/G		0.85 ± 0.05	0.92 ± 0.05	0.89 ± 0.07	0.91 ± 0.11	0.87 ± 0.04	1.01 ± 0.09*

Values are given as the mean ± S.D.
*: Significantly different from the control, $p \leqq 0.05$. **: Significantly different from the control, $p \leqq 0.01$.

pression of body weight gain in females during pregnancy was not observed, the lowered body weight on PND 0 was considered a direct effect of PFUA due to intrauterine exposure. Also in other PFCAs, low values of body weight of pups at birth without effects on the body weight of dams in the gestation period were observed (Butenhoff *et al.*, 2004; Loveless *et al.*, 2009). The lowered body weight on PND 4 was considered to be a direct effect of PFUA by ingestion of breast milk, as well as a secondary effect of PFUA caused by the lowered body weight in

Table 3. Organ weights

		Main Group				Satellite Group	
Dose (mg/kg/day)		0 (control)	0.1	0.3	1.0	0 (control)	1.0
Males							
No. of animals examined		5	5	5	5	5	5
Brain	(g)	2.18 ± 0.08	2.18 ± 0.09	2.15 ± 0.08	2.17 ± 0.08	2.09 ± 0.04	2.14 ± 0.13
	(%)[a]	0.42 ± 0.03	0.4 ± 0.03	0.41 ± 0.01	0.44 ± 0.05	0.39 ± 0.03	0.44 ± 0.03**
Throid[b]	(mg)	22.4 ± 1.8	25.7 ± 2.5	21.1 ± 2.9	22.3 ± 3.5	23.5 ± 3.8	18.7 ± 2.9
	(%)[a]	4.3 ± 0.4	4.7 ± 0.4	4.1 ± 0.6	4.5 ± 0.7	4.4 ± 0.5	3.8 ± 0.4
Thymus	(mg)	297 ± 90	432 ± 173	342 ± 106	260 ± 61	250 ± 80	251 ± 67
	(%)[a]	57 ± 19	79 ± 27	66 ± 21	53 ± 16	47 ± 17	51 ± 11
Heart	(g)	1.52 ± 0.1	1.5 ± 0.2	1.51 ± 0.03	1.38 ± 0.17	1.46 ± 0.17	1.29 ± 0.19
	(%)[a]	0.29 ± 0.02	0.28 ± 0.04	0.29 ± 0	0.28 ± 0.02	0.28 ± 0.02	0.27 ± 0.02
Liver	(g)	15.12 ± 2.14	16.45 ± 2.06	17.54 ± 0.73	20.95 ± 2.56**	14.19 ± 1.56	19.85 ± 3.03**
	(%)[a]	2.88 ± 0.27	3.02 ± 0.19	3.39 ± 0.16**	4.18 ± 0.19**	2.67 ± 0.22	4.07 ± 0.36**
Spleen	(g)	0.84 ± 0.16	0.76 ± 0.09	0.79 ± 0.05	0.65 ± 0.09*	0.72 ± 0.11	0.72 ± 0.04
	(%)[a]	0.16 ± 0.03	0.14 ± 0.01	0.15 ± 0.01	0.13 ± 0.01*	0.14 ± 0.02	0.15 ± 0.01
Kidney[b]	(g)	3.43 ± 0.31	3.44 ± 0.38	3.51 ± 0.08	3.4 ± 0.17	3.51 ± 0.31	3.32 ± 0.43
	(%)[a]	0.65 ± 0.06	0.63 ± 0.04	0.68 ± 0.03	0.68 ± 0.06	0.66 ± 0.03	0.68 ± 0.04
Adrenal[b]	(mg)	64 ± 13	70 ± 8	68 ± 3	58 ± 9	61 ± 9	46 ± 8*
	(%)[a]	12 ± 2	13 ± 1	13 ± 1	12 ± 1	12 ± 2	9 ± 1
Testis[b,c]	(g)	3.34 ± 0.21	3.57 ± 0.26	3.48 ± 0.28	2.98 ± 0.86	3.49 ± 0.26	3.57 ± 0.35
	(%)[a]	0.63 ± 0.07	0.67 ± 0.05	0.68 ± 0.06	0.62 ± 0.17	0.66 ± 0.03	0.74 ± 0.07*
Epididymis[b,c]	(mg)	1339 ± 84	1420 ± 112	1368 ± 199	1578 ± 950	1337 ± 51	1388 ± 87
	(%)[a]	252 ± 21	265 ± 25	268 ± 36	335 ± 220	252 ± 11	288 ± 34
Females							
No. of animals examined		5	5	5	5	5	5
Brain	(g)	1.99 ± 0.05	1.97 ± 0.08	1.98 ± 0.09	2 ± 0.04	1.96 ± 0.09	1.86 ± 0.06
	(%)[a]	0.64 ± 0.04	0.66 ± 0.03	0.65 ± 0.05	0.67 ± 0.06	0.68 ± 0.08	0.78 ± 0.02**
Throid[b]	(mg)	17.2 ± 1.8	19.2 ± 3.2	17.5 ± 3	16.9 ± 0.7	17.2 ± 2.7	14.7 ± 1
	(%)[a]	5.5 ± 0.8	6.5 ± 1.1	5.8 ± 1.1	5.6 ± 0.6	6 ± 1	6.2 ± 0.3
Thymus	(mg)	192 ± 16	170 ± 102	243 ± 82	249 ± 58	245 ± 98	147 ± 59
	(%)[a]	61 ± 4	56 ± 32	79 ± 24	82 ± 14	85 ± 39	62 ± 23
Heart	(g)	1.02 ± 0.08	0.96 ± 0.06	0.92 ± 0.04	0.94 ± 0.11	0.86 ± 0.05	0.73 ± 0.03**
	(%)[a]	0.33 ± 0.03	0.32 ± 0.01	0.3 ± 0.01	0.31 ± 0.02	0.29 ± 0.02	0.31 ± 0.01
Liver	(g)	10.56 ± 0.68	10.61 ± 0.48	10.55 ± 1.48	12.76 ± 1.00**	7.22 ± 0.38	8.63 ± 1.04*
	(%)[a]	3.37 ± 0.12	3.57 ± 0.13	3.46 ± 0.36	4.21 ± 0.15**	2.48 ± 0.14	3.64 ± 0.47**
Spleen	(g)	0.62 ± 0.06	0.65 ± 0.16	0.65 ± 0.1	0.66 ± 0.15	0.49 ± 0.05	0.43 ± 0.05
	(%)[a]	0.2 ± 0.02	0.22 ± 0.05	0.22 ± 0.02	0.21 ± 0.03	0.17 ± 0.02	0.18 ± 0.01
Kidney[b]	(g)	2.24 ± 0.42	1.96 ± 0.18	2.06 ± 0.19	2.05 ± 0.09	1.89 ± 0.14	1.93 ± 0.17
	(%)[a]	0.72 ± 0.14	0.66 ± 0.06	0.68 ± 0.07	0.68 ± 0.04	0.64 ± 0.02	0.81 ± 0.07**
Adrenal[b]	(mg)	82 ± 4	84 ± 10	89 ± 14	80 ± 13	70 ± 8	49 ± 5**
	(%)[a]	26 ± 2	28 ± 5	30 ± 5	26 ± 3	25 ± 5	21 ± 1

Values are given as the mean ± S.D.

[a]: Ratio of organ weight to body weight (relative organ weight). [b]: Values are represented as the total weights of the organs on both sides. [c]: Organ weight was measured for all animals (number of examined animals: 7 at 0 and 1.0 mg/kg/day and 12 at 0.1 and 0.3 mg/kg/day in the main group, and 5 at 0 and 1.0 mg/kg/day in the recovery group.)

*: Significantly different from the control, $p \leqq 0.05$. **: Significantly different from the control, $p \leqq 0.01$.

Table 4. Histopathological findings

	Males						Females					
	Main				Satellite		Main				Satellite	
Dose (mg/kg/day)	0	0.1	0.3	1.0	0	1.0	0	0.1	0.3	1.0	0	1.0
Heart												
Number examined	5	0	0	5			5	0	0	5		
Cardiomyopathy (minimal)	1			1			0			0		
Kidney												
Number examined	5	0	1	5			5	0	0	5		1
Dilatation, pelvic	0		1	0			1			0		1
(minimal)			1									1
(moderate)							1					
Regeneration, tubular	4		1	1			1			1		0
(minimal)	3		1	1			1			1		
(mild)	1											
Liver												
Number examined	7	12	12	7	5	5	12	12	12	12	5	5
Vacuolation, hepatocytes, diffuse	0	0	0	3	0	1	0	0	0	0	0	0
(minimal)				2		1						
(mild)				1								
Necrosis, focal (minimal)	0	0	0	2	0	0	0	0	0	2	0	0
Cell infiltration, Glisson's sheath (mild)	0	0	0	0	0	0	0	0	0	0	0	2
Microgranuloma	4	3	1	2	3	3	1	1	0	2	4	4
(minimal)	4	3	1	2	3	3	1	1		2	4	2
(mild)												2
Degeneration, hepatocytes, centrilobular (minimal)	0	0	0	0	0	3	0	0	0	0	0	3
Hypertrophy, hepatocytes, centrilobular	0	0	3	7	0	5	0	0	1	11	0	5
(minimal)			2						1	8		
(mild)			1	2		3				3		2
(moderate)				5		2						3
Spleen												
Number examined	5	0	0	5			5	0	0	5		
Hematopoiesis, extramedullary (minimal)	4			1			5			4		
Stomach												
Number examined	7	12	12	7	5	5	6	0	0	5		
Erosion, glandular stomach (minimal)	0	0	0	3	0	0	2			0		
Thymus												
Number examined	5	0	0	5			5	1	0	5		
Atrophy, lymphoid (mild)	0			0			0	1		0		
Thyroid												
Number examined	5	0	0	5			5	0	0	5		
Ectopic thymus (minimal)	0			0			0			1		
Cyst, ultimobranchial (minimal)	1			2			2			0		
Testis												
Number examined	5	0	0	5								
Not remarkable	5			5								
Epididymis												
Number examined	5	1	0	5								
Granuloma, spermatic	1	1		1								
(minimal)		1		1								
(mild)	1											
Uterus												
Number examined							5	1	0	5		
Dilatation, lumina (minimal)							0	1		0		

Table 5. Reproductive and developmental parameters

	0 mg/kg/day	0.1 mg/kg/day	0.3 mg/kg/day	1.0 mg/kg/day
Number of animals (males/females)	12/12	12/12	12/12	12/12
Copulation index (males/females) (%)	100/100	100/100	100/100	100/100
Fertility index (%)	100	91.7	100	100
Gestation index (%)	100	100	100	100
Number of pregnant animals	12	11	12	12
Gestation length (days)	22.0 ± 0.3	22.1 ± 0.5	22.1 ± 0.5	21.7 ± 0.2
Number of corpora lutea	15.8 ± 1.9	16.8 ± 1.8	16.2 ± 1.9	16.2 ± 1.5
Number of implantation sites	14.6 ± 2.0	15.5 ± 3.3	15.0 ± 1.9	15.3 ± 1.6
Implantation index (%)	92.0 ± 5.5	91.0 ± 15.4	92.8 ± 6.0	94.8 ± 4.4
Number of litters	12	11	12	12
Number of live pups on PND 0	13.9 ± 2.2	14.5 ± 3.4	13.1 ± 3.1	13.5 ± 2.2
Live birth index (%)	98.9 ± 2.6	97.3 ± 5.3	93.2 ± 18.2	97.9 ± 4.1
Sex ratio	0.51	0.47	0.55	0.52
Number of live pups on PND 4	13.7 ± 1.9	14.0 ± 3.2	12.8 ± 3.1	13.4 ± 2.2
Viability index (%)	98.5 ± 2.8	97.1 ± 3.3	97.7 ± 5.9	99.4 ± 2.2
Body weight of male pups (g)				
on PND 0	6.7 ± 0.3	6.7 ± 0.6	6.4 ± 0.5	5.8 ± 0.3**
on PND 4	10.5 ± 0.5	10.1 ± 1.8	10.2 ± 1.2	8.5 ± 0.7**
Body weight of female pups (g)				
on PND 0	6.4 ± 0.4	6.3 ± 0.6	6.1 ± 0.6	5.6 ± 0.2**
on PND 4	9.9 ± 0.6	9.7 ± 1.7	9.5 ± 0.8	8.3 ± 0.7**

Values are given as the mean ± S.D.
**: Significantly different from the control, $p \leqq 0.01$.

dams. In the PFOA oral dose study (Abbott *et al.*, 2007), the reduction of postnatal weight gain appeared to depend on PPARα expression.

The elimination rate of PFOA in female rats is approximately 40 times faster than in male rats (ATSDR, 2009). Organic anion transport proteins play a key role in PFCAs (C4 to C10) renal tubular reabsorption (Han *et al.*, 2012), and the slower elimination of PFOA in male rats compared to female rats has been attributed to sex hormone modulation of organic anion transporters in the kidney (ATSDR, 2009). In the present study, there were slight gender differences in the hepatotoxicity of PFUA: liver weight increased in males at 0.3 mg/kg/day and above and in females at 1.0 mg/kg/day, and histopathological findings observed in the 1.0 mg/kg/day groups were more numerous and severer in males than in females. The gender differences in hepatotoxicity observed in the present study are considered to be attributable to faster elimination in female rats, as with other PFCAs.

Increased liver weight and hepatocellular hypertrophy, induced by activation of PPARα, were generally observed in previous studies on PFAAs. Significant peroxisome proliferative activity seems to require a carbon length more than 7 (ATSDR, 2009). In gavage studies of PFAAs in male rats, which are more sensitive than females, the following results were observed; for PFOA (C8), increased liver weight and hepatocellular hypertrophy at 5 mg/kg/day for 28 days (Cui *et al.*, 2009); for perfluorononanoic acid (C9), increased liver weight at 1 mg/kg/day for 14 days (Fang *et al.*, 2012); for perfluorododecanoic acid (C12), increased liver weight at 0.02 mg/kg/day for 110 days (Ding *et al.*, 2009). In the current study of PFUA (C11), increased liver weight and centrilobular hypertrophy of hepatocytes were observed from 0.3 mg/kg/day for 42 days. In consideration of differences in the administration period or doses in these studies, the intensity of the liver toxicity of PFUA (C11) was estimated to be between C9 and C12, suggesting that the toxic potency of PFAAs (C8-C12) increases by lengthening their carbon chain. This is because hydrophobicity, which increases as carbon length increases, seems to favor biliary enterohepatic recirculation, resulting in more protracted toxicity (ATSDR, 2009). In contrast, 42-day administration of PFOdA (C18) increased liver

weight at 200 mg/kg/day but not at 40 mg/kg/day in male rats (Hirata-Koizumi *et al.*, 2012). In comparison with other PFAAs (C8-C12), including PFUA (C11), PFOdA induced liver toxicity at higher doses, and this may be due to the low absorption of PFOdA into the body.

At 1.0 mg/kg/day in the main group, the following effects on hematological and blood biochemical parameters were observed; a decrease in fibrinogen was observed in males and females, but increases in APTT and PT were not observed, suggesting that there would be no toxicologically significant effects on the blood coagulation system; decreases in fibrinogen, total protein and albumin observed in males and/or females may be due to reduced synthesis in the damaged liver; the increase in BUN observed in males and females could be due to increased hepatic protein catabolism, because urinalysis parameters and the gross and microscopic appearance of the kidneys were not changed; and the increase of ALP in males was related to the histopathological findings in the liver. These effects except for the decrease in fibrinogen in females were observed also at the end of the recovery period, and the increase of ALP was observed in females only after the recovery period. Moreover, in histopathological findings, centrilobular degeneration of hepatocytes in both sexes and Glisson's sheath cell infiltration in females were observed only at the end of the recovery period, and in females, centrilobular hypertrophy of hepatocytes was more serious at the end of the recovery period. These results suggest that the whole body elimination of PFUA in rats, as well as other PFCAs, is slow. There are some reports indicating that PFCAs are secreted in bile and undergo extensive reabsorption from the gastrointestinal tract (Kudo *et al.*, 2001; Vanden Heuvel *et al.*, 1991a, 1991b; reviewed in ATSDR, 2009). In general, PFCAs with longer carbon chains (C4-C10) have a longer half-life (Hirata-Koizumi *et al.*, 2012). Although the elimination half-life of PFUA is unknown, the half-life after intravenous injection of perfluorodecanoic acid (PFDeA, C10) in rats was about 40 to 60 days (Ohmori *et al.*, 2003), It is estimated that the half-life of PFUA is longer than the recovery period, 14 days, and it is reasonable that some effects of PFUA appear after the recovery period. The above findings may be effects of PFUA caused by enterohepatic recirculation, which lasted through the dosing and recovery periods. The decrease in grip strength of the forefoot observed in males and females at 1.0 mg/kg/day in the satellite group was considered a secondary effect related to suppression of body weight gain.

In conclusion, the NOAEL for repeated dose toxicity is considered to be 0.1 mg/kg/day based on the observed centrilobular hypertrophy of hepatocytes in both sexes at 0.3 mg/kg/day, and the NOAEL for reproductive/developmental toxicity is considered to be 0.3 mg/kg/day based on the lowered body weight of pups at birth and body weight gain at 4 days after birth inhibited at 1.0 mg/kg/day.

ACKNOWLEDGMENTS

This study was undertaken under the Japanese safety programme for existing chemicals funded by the Ministry of Health, Labour and Welfare, Japan, and was supported by a Health and Labour Sciences Research Grant (H22-Kenki-Ippan-006, H25-Kenki-Ippan-007) from the Ministry of Health, Labour and Welfare, Japan.

REFERENCES

Abbott, B.D., Wolf, C.J., Schmid, J.E., Das, K.P., Zehr, R.D., Helfant, L., Nakayama, S., Lindstrom, A.B., Strynar, M.J. and Lau, C. (2007): Perfluorooctanoic acid-induced developmental toxicity in the mouse is dependent on expression of peroxisome proliferator-activated receptor-alpha. Toxicol. Sci., **98**, 571-581.

ATSDR (2009): Toxicological profile for Perfluoroalkyls (Draft for Public Comment). U.S. Department of health and human services, Public health service, Agency for Toxic Substances and Disease Registry (ATSDR). May 2009.

Butenhoff, J.L., Kennedy, G.L.Jr., Frame, S.R., O'Connor, J.C. and York, R.G. (2004): The reproductive toxicology of ammonium perfluorooctanoate (APFO) in the rat. Toxicology, **196**, 95-116.

Calafat, A.M., Needham, L.L., Kuklenyik, Z., Reidy, J.A., Tully, J.S., Aguilar-Villalobos, M. and Naeher, L.P. (2006): Perfluorinated chemicals in selected residents of the American continent. Chemosphere, **63**, 490-496.

Calafat, A.M., Kuklenyik, Z., Reidy, J.A., Caudill, S.P., Tully, J.S. and Needham, L.L. (2007a): Serum concentrations of 11 polyfluoroalkyl compounds in the U.S. population: Data from the National Health and Nutrition Examination Survey (NHANES) 1999-2000. Environ. Sci. Technol., **41**, 2237-2242.

Calafat, A.M., Wong, L.Y., Kuklenyik, Z., Reidy, J.A. and Needham, L.L. (2007b): Polyfluoroalkyl chemicals in the U.S. population: Data from the National Health and Nutrition Examination Survey (NHANES) 2003-2004 and comparisons with NHANES 1999-2000. Environ. Health Perspect., **115**, 1596-1602.

CHRIP (2013): Chemical Risk Information Platform. Available at: http://www.safe.nite.go.jp/japan/db.html, accessed in March and October 2013, or at: http://www.meti.go.jp/policy/chemical_management/kasinhou/information/volume_index.html.

Cui, L., Zhou, Q.F., Liao, C.Y., Fu, J.J. and Jiang, G.B. (2009): Studies on the toxicological effects of PFOA and PFOS on rats using histological observation and chemical analysis. Arch. Environ. Contam. Toxicol., **56**, 338-349.

Ding, L., Hao, F., Shi, Z., Wang, Y., Zhang, H., Tang, H. and Dai, J. (2009): Systems biological responses to chronic perfluorododecanoic acid exposure by integrated metabonomic and transcriptomic studies. J. Proteome Res., **8**, 2882-2891.

Domingo, J.L., Ericson-Jogsten, I., Eriksson, U., Martorell, I., Perelló, G., Nadal, M. and van Bavel, B. (2012): Human dietary exposure to perfluoroalkyl substances in Catalonia, Spain. Tem-

poral trend. Food Chem., **135**, 1575-1582.
ECHA (2012): European Chemicals Agency. Member state committee, support document for identification of Henicosafluoroundecanoic Acid as a substance of very high concern because of its vPvB properties. Adopted on 13 December 2012.
Environment Canada (2010): Draft ecological screening assessment report. Long-chain (C9-C20) Perfluorocarboxylic acids, their salts and their precursors. October 2010.
EPA (2013a): U.S. Environmental Protection Agency. Perfluorooctanoic Acid (PFOA) and Fluorinated Telomers. Available at: http://www.epa.gov/opptintr/pfoa/index.html, accessed in Mar 2013.
EPA (2013b): U.S. Environmental Protection Agency. PFOA Stewardship Program Reporting Guidance. Available at: http://www.epa.gov/opptintr/pfoa/pubs/stewardship/pfoaguidance.html#minimize. accessed in Mar 2013.
Fang, X., Zou, S., Zhao, Y., Cui, R., Zhang, W., Hu, J. and Dai, J. (2012): Kupffer cells suppress perfluorononanoic acid-induced hepatic peroxisome proliferator-activated receptor α expression by releasing cytokines. Arch. Toxicol., **86**, 1515-1525.
Han, X., Nabb, D.L., Russell, M.H., Kennedy, G.L. and Rickard, R.W. (2012): Renal elimination of perfluorocarboxylates (PFCAs). Chem. Res. Toxicol., **25**, 35-46.
Hinderliter, P.M., Mylchreest, E., Gannon, S.A., Butenhoff, J.L. and Kennedy, G.L.Jr. (2005): Perfluorooctanoate: Placental and lactational transport pharmacokinetics in rats. Toxicology, **211**,139-148.
Hirata-Koizumi, M., Fujii, S., Furukawa, M., Ono, A. and Hirose, A. (2012): Repeated dose and reproductive/developmental toxicity of perfluorooctadecanoic acid in rats. J. Toxicol. Sci., **37**, 63-79.
IARC (1995). Peroxisome Proliferation and its Role in Carcinogenesis. International Agency for Research on Cancer (IARC), Working Group of 7-11 December 1994, Report N° 24, Lyon, France. 11.
Japanese law (2005): Act on Welfare and Management of Animals. Act No.105 of October 1, 1973. As amended up to Act No.68 of June 22, 2005.
Japanese law (2009): Act on the Evaluation of Chemical Substances and Regulation of Their Manufacture, etc. Law number: Act No. 117 of 1973. Amendment: Act No.39 of 2009.
Kudo, N., Suzuki, E., Katakura, M., Ohmori, K., Noshiro, R. and Kawashima, Y. (2001): Comparison of the elimination between perfluorinated fatty acids with different carbon chain length in rats. Chem. Biol. Interact., **134**, 203-216.
Kuklenyik, Z., Reich, J.A., Tully, J.S., Needham, L.L. and Calafat, A.M. (2004): Automated solid-phase extraction and measurement of perfluorinated organic acids and amides in human serum and milk. Environ. Sci. Technol., **38**, 3698-3704.
Lau, C., Anitole, K., Hodes, C., Lai, D., Pfahles-Hutchens, A. and Seed, J. (2007): Perfluoroalkyl acids: a review of monitoring and toxicological findings. Toxicol. Sci., **99**, 366-394.
Loveless, S.E., Slezak, B., Serex, T., Lewis, J., Mukerji, P., O'Connor, J.C., Donner, E.M., Frame, S.R., Korzeniowski, S.H. and Buck, R.C. (2009): Toxicological evaluation of sodium perfluorohexanoate. Toxicology, **264**, 32-44.
MOE, METI and MHLW (2003): Standard concerning testing laboratories implementing tests for new chemical substances etc. Joint notification by director generals of Environmental Policy Bureau, Japan, Ministry of the Environment (MOE) (Kanpokihatsu No 031121004) and Manufacturing Industries Bureau, Ministry of Economy, Trade and Industry (METI) (Seikyokuhatsu No 3), dated November 17, 2003 and by director general of Pharmaceutical and Food Safety Bureau, Ministry of Health, Labour and Welfare (MHLW) (Yakusyokuhatsu No 1121003), dated November 21, 2003.
MOE, METI and MHLW (2008): Partial amendments of the standard concerning testing laboratories implementing tests for new chemical substances etc. Joint notification by director generals of Environmental Policy Bureau, Japan, Ministry of the Environment (MOE) (Kanpokihatsu No 080704001) and Manufacturing Industries Bureau, Ministry of Economy, Trade and Industry (METI) (Seikyokuhatsu No 2), dated June 30, 2008 and by director general of Pharmaceutical and Food Safety Bureau, Ministry of Health, Labour and Welfare (MHLW) (Yakusyokuhatsu No 0704001), dated July 4, 2008.
Ohmori, K., Kudo, N., Katayama, K. and Kawashima, Y. (2003): Comparison of the toxicokinetics between perfluorocarboxylic acids with different carbon chain length. Toxicology, **184**, 135-140.
Peters, J.M. and Gonzalez, F.J. (2011): Why toxic equivalency factors are not suitable for perfluoroalkyl chemicals. Chem. Res. Toxicol., **24**, 1601-1609.
So, M.K., Yamashita, N., Taniyasu, S., Jiang, Q., Giesy, J.P., Chen, K. and Lam, P.K. (2006): Health risks in infants associated with exposure to perfluorinated compounds in human breast milk from Zhoushan, China. Environ. Sci. Technol., **40**, 2924-2929.
Vanden Heuvel, J.P., Kuslikis, B.I., Shrago, E. and Peterson, R.E. (1991a): Inhibition of long-chain acyl-CoA synthetase by the peroxisome proliferator perfluorodecanoic acid in rat hepatocytes. Biochem. Pharmacol., **42**, 295-302.
Vanden Heuvel, J.P., Kuslikis, B.I., Van Rafelghem, M.J. and Peterson, R.E. (1991b): Disposition of perfluorodecanoic acid in male and female rats. Toxicol. Appl. Pharmacol., **107**, 450-459.
Vestergren, R., Berger, U., Glynn, A. and Cousins, I.T. (2012): Dietary exposure to perfluoroalkyl acids for the Swedish population in 1999, 2005 and 2010. Environ. Int., **49**, 120-127.
Wolf, C.J., Schmid, J.E., Lau, C. and Abbott, B.D. (2012): Activation of mouse and human peroxisome proliferator-activated receptor-alpha (PPARα) by perfluoroalkyl acids (PFAAs): further investigation of C4-C12 compounds. Reprod. Toxicol., **33**, 546-551.

Separation and Purification Technology 107 (2013) 79–84

Contents lists available at SciVerse ScienceDirect

Separation and Purification Technology

journal homepage: www.elsevier.com/locate/seppur

Adsorptive virus removal with super-powdered activated carbon

Taku Matsushita *, Hideaki Suzuki, Nobutaka Shirasaki, Yoshihiko Matsui, Koichi Ohno

Graduate School of Engineering, Hokkaido University, N13W8, Sapporo 060-8628, Japan

ARTICLE INFO

Article history:
Received 17 April 2012
Received in revised form 10 January 2013
Accepted 15 January 2013
Available online 31 January 2013

Keywords:
Bacteriophage
Drinking water treatment
Hydrophobicity
Zeta potential

ABSTRACT

We investigated the removal of bacteriophages by adsorption on commercially available powdered activated carbon (N-PAC, median diameter >10 μm) and super-powdered activated carbon (S-PAC, median diameter 0.7–2.8 μm). N-PACs failed to remove the virus in Milli-Q water buffered with 100 μM Ca^{2+}, but some S-PACs successfully removed it under the same condition. Three factors contributed substantially to virus removal: a smaller electrophoretic repulsive force between the virus and the PAC particles, a large proportion of pores 20–50 nm in diameter, and a greater hydrophobicity of the virus surface.

1. Introduction

The development of detection techniques based on molecular biology has enabled us to detect fragments of viral genomes in environmental waters, including drinking water sources, highlighting the need to ensure the removal of viruses at drinking water treatment plants. Although disinfecting water with hypochlorite ensures the biological safety of the finished water, the risk of virus infections can be reduced by physicochemical treatments such as coagulation–sedimentation–sand filtration; physical sieving processes such as ultrafiltration, nanofiltration, and reverse osmosis; and ozonation and UV irradiation.

Activated carbon adsorption is widely used to treat drinking water in Japan. Granular activated carbon (GAC) is used in combination with ozonation for removing byproducts derived from the oxidative decomposition of organic matter. Powdered activated carbon (PAC) is seasonally applied with excellent results for removing chemicals with an earthy–musty odor and pesticides. It has also been tested for virus removal. Adsorption experiments with a GAC-loaded (20 × 50 mesh, equivalent to 297–853 μm) column-type reactor removed only 24–50% of poliovirus [1]. Worse, GAC filtration did not remove bacteriophage MS2 [2]. These results indicate that GAC is not suitable for substantial virus removal within the contact time allowed in actual drinking water treatment, probably on account of a low rate of adsorption of virus. Indeed, only 70% of bacteriophage T4 was removed by activated carbon (300–425 μm) after 2 h of contact time [3]. Accordingly, effective virus removal by activated carbon will require a longer contact time, an extremely high dose of activated carbon, or both.

Reducing the particle size of activated carbon increases the rate of adsorption [4,5], because the travel distance for intraparticle radial diffusion is reduced and the specific surface area per adsorbent mass is increased [6]. Pulverizing activated carbon would therefore overcome the problems of slow adsorption kinetics, but the PAC particle size was previously limited to about 5 μm. Recent advances in nanotechnology now enable pulverization down to submicron or nanometer size ranges at a reasonable cost, producing super-powdered activated carbon (S-PAC) [7–9]. As S-PAC might improve virus removal, our objectives were to investigate the effect of pulverization of PAC particles on virus removal and the factors contributing to virus removal.

2. Materials and methods

2.1. Activated carbon

We tested 11 commercially available, thermally activated, normal PACs (N-PACs): 9 wood-based, 2 coconut-based, and 1 coal-based (Table 1). To prepare the S-PACs, we ground the N-PACs in a wet bead mill (Metawater Co., Ltd., Tokyo, Japan). We used both sets of materials to determine the effects of particle size on virus removal by adsorption. The PACs were dried in an oven at 105 °C and stored in a desiccator before use. They were then made into 5% slurries in Milli-Q water (Milli-Q Advantage, Millipore Corp., Billerica, MA, USA) and placed under vacuum to remove any air from the pores. The slurries were stored at 4 °C before dilution for use in the experiments. The particle size distributions were determined by laser scattering (LMS-30 Micron Sizer; Seishin Enterprise Co., Ltd., Tokyo, Japan). The surfaces of the N-PACs were observed by scanning transmission electron microscopy (SEM, JSM-7400F; JEOL Ltd., Tokyo, Japan).

* Corresponding author. Tel./fax: +81 11 706 7279.
E-mail address: taku-m@eng.hokudai.ac.jp (T. Matsushita).

1383-5866/$ - see front matter © 2013 Published by Elsevier B.V.
http://dx.doi.org/10.1016/j.seppur.2013.01.017

Table 1
Activated carbon used.

	Raw material	Median diameter (μm)		Key characteristics of S-PAC						
				Specific surface area[a] (m^2/g)	Element contents[b] (%)				Functional group[c]	
		S-PAC	N-PAC		C	O	N	S	Acidic	Basic
Wood-1	Wood	0.69	13.24	1145 ± 33	85.3 ± 0.6	7.05 ± 0.97	0.14 ± 0.01	0.10 ± 0.02	350 ± 9	790 ± 21
Wood-2	Wood	0.83	4.5	873 ± 39	80.0 ± 1.5	6.70 ± 0.51	0.25 ± 0.02	0.20 ± 0.02	193 ± 58	711 ± 139
Wood-3	Wood	1.49	NA	NA	NA	NA	NA	NA	NA	NA
Wood-4	Wood	0.66	NA	NA	84.6 ± 0.8	6.72 ± 0.11	0.15 ± 0.00	0.11 ± 0.03	NA	NA
Wood-5	Wood	2.79	NA	NA	NA	NA	NA	NA	NA	NA
Wood-6	Wood	1.38	NA	NA	NA	NA	NA	NA	NA	NA
Wood-7	Wood	2.20	NA	NA	NA	NA	NA	NA	NA	NA
Wood-8	Wood	0.93	11.46	1174 ± 14	81.9 ± 0.6	8.24 ± 0.48	0.20 ± 0.01	0.15 ± 0.02	351 ± 22	780 ± 56
Wood-9	Wood	1.65	0.6	NA	NA	NA	NA	NA	NA	NA
Coconut-1	Coconut shell	0.67	NA	NA	88.1 ± 0.5	5.95 ± 0.41	0.16 ± 0.02	0.11 ± 0.03	425 ± 34	329 ± 35
Coconut-2	Coconut shell	0.65	19.13	1215 ± 149	89.1 ± 0.2	5.30 ± 0.10	0.18 ± 0.04	0.06 ± 0.02	433 ± 16	582 ± 29
Coal-1	Coal	0.67	NA	NA	79.2 ± 0.3	10.62 ± 0.24	0.38 ± 0.00	0.55 ± 0.01	757 ± 36	366 ± 36
Determination coefficient (r^2) between logarithmic virus removal indicated in Fig. 2				0.38	0.01	0.06	0.06	0.06	0.08	0.10

NA – not applicable.
[a] Determined with BET.
[b] Measured with an elemental analyzer (Vario EL III, Elementar Analysensysteme GmbH, Hanau, Germany).
[c] Measured with Boehm titration [28,29].

2.2. Viruses

As model viruses we used two bacteriophages, Qβ (NBRC 20012) and MS2 (NBRC 20015), obtained from the Biological Resource Center (NBRC) of the National Institute of Technology and Evaluation (Chiba, Japan). The diameters of Qβ and MS2 are 23.5 ± 0.8 nm and 22.5 ± 1.0 nm, respectively [10]. The viruses were propagated for 22–24 h at 37 °C in *Escherichia coli* F^+ (NBRC 13965) obtained from NBRC. The cultures were centrifuged at 3000*g* for 10 min and then filtered through a 0.45-μm pore-size membrane (cellulose acetate; DISMIC-25cs; Toyo Roshi Kaisya, Ltd., Tokyo, Japan). The filtrate was purified twice in a centrifugal filter device (molecular weight cutoff: 100,000; Centriplus-100; Millipore Corp., Billerica, MA, USA) to prepare virus stock solution. Virus concentrations were measured by the plaque-forming unit (PFU) method according to the agar overlay method [11] using the bacterial host *E. coli* F^+. Average plaque counts of triplicate plates prepared from one sample gave the virus concentration.

2.3. Batch adsorption test

Milli-Q water was buffered with 424 μM $NaHCO_3$ to give the equivalent of 20 mg-$CaCO_3$/L of alkalinity (buffered Milli-Q water). The buffered Milli-Q water was supplemented with 0, 100, 200, 300, 400, or 500 μM $CaCl_2$. In a square beaker, 500 mL of solution was adjusted to pH 6.8 with HCl, and either Qβ or MS2 was added to give 10^6 PFU/mL. PAC was added at 20 mg/L and the suspension was continuously stirred at $G = 200\ s^{-1}$ with a jar tester. Samples were withdrawn at 0, 1, 2, 4, and 8 h and filtered through a membrane (ϕ = 0.2 μm, PTFE; Toyo Roshi Kaisya) to remove the PAC particles. The virus concentration in the permeate was measured by the PFU method.

2.4. Electrophoretic mobility

All solutions were held for 1 day at 20 °C for the pH to stabilize. Just before measurement, each S-PAC or virus was suspended in the solution at ~20 mg/L or 10^9 PFU/mL, respectively. The electrophoretic mobility of S-PACs and viruses was measured with an electrophoretic light-scattering spectrophotometer (Zetasizer Nano ZS, 532 nm green laser; Malvern Instruments Ltd., Malvern, Worcestershire, UK) at 25 °C and at a 17° measurement angle.

2.5. Pore size distribution analyses of PACs

Pore size was analyzed by nitrogen gas adsorption at 77 K with an automated gas sorption analyzer (Autosorb-iQ-MP; Quantachrome Instruments, Boynton Beach, FL, USA). Pore size distributions were determined by a combination of two widely accepted models: the DFT model for the pore size distribution of micropores (<2 nm) and the BJH theory for the volumes of mesopores and macropores (>2 nm).

2.6. Virus hydrophobicity

Hydrophobicity was estimated by the bacterial adhesion to hydrocarbon (BATH) method [12]. Virus was added to 3 mL of buffered Milli-Q water at a final concentration of ~10^8 PFU/mL at pH 7.0. The solution was supplemented with 0.25 mL of solvent (*n*-hexadecane, *n*-octane, or *p*-xylene). The solution was intensely vortexed for 2 min, and then rested for 15 min at room temperature to allow the solvent and water to separate. The virus concentration in the water phase was measured by real-time PCR [13]. A decrease in virus concentration was used as a measure of the virus surface hydrophobicity [12].

3. Results and discussion

3.1. Comparison of virus removal between N-PACs and S-PACs

Virus removal increased with time even without PAC dosing (black circles), probably owing to spontaneous inactivation (Fig. 1). N-PACs (white circles) of wood-8 and coconut-2 showed the same result as the control. S-PACs of wood-8 and coconut-2 (gray circles) also showed the same result, even though their outer surface areas per unit mass were 12.3× and 29.4× those of the N-PACs, respectively. N-PAC of wood-1 removed some virus. In contrast, S-PAC of wood-1, with 19.2× the outer surface area of the N-PAC, caused a monotonic decrease in virus concentration with contact time, reaching a 4 log reduction after 8 h. Our result appears to disagree with that of Powell et al. [14], who reported

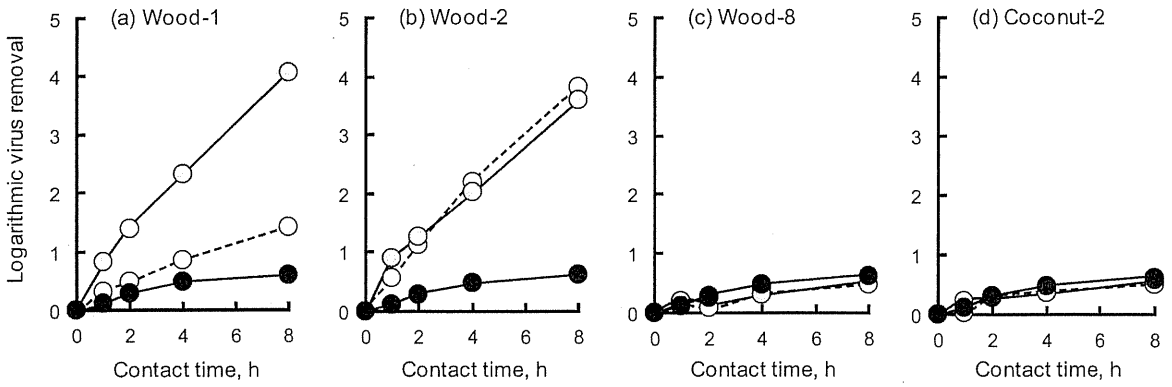

Fig. 1. Changes in virus (Qβ) removal with contact time (Ca^{2+} = 100 μM). Gray, white and black circles indicate SPAC, N-PAC and control, respectively.

that the adsorption of bacteriophage MS2 to a GAC reached equilibrium in 3 h. However, whereas they found that the amount of virus *adsorbed* had plateaued (>99% removal), we monitored the concentration of virus in the *liquid phase*, which might have decreased further even after 99% of the virus was adsorbed. N-PAC of wood-2 removed virus at the same extent as S-PAC of wood-1, possibly because the particle size of N-PAC of wood-2 was much smaller than those of other N-PACs. Virus removal with S-PAC of wood-2 was almost the same to that with the N-PAC, possibly because the N-PAC was small enough to remove the virus and its outer surface area was not so much increased with the pulverization (5.4×). The pulverization enhanced the adsorptive removal by the wood-1 PAC, but not by the wood-2, wood-8 and coconut-2 PACs. Overall, the effect of pulverization on virus removal might depend on the intrinsic characteristics of the PACs.

3.2. Effects of median diameter and PAC source on virus removal

We expected that finer PACs would remove more virus. However, different S-PACs with the same median diameter of ~0.7 μm showed very different removals of virus: wood-1 and wood-2 S-PACs achieved a removal of ~4 orders of magnitude (4 logs), whereas the other S-PACs achieved a removal of <2 logs (Fig. 2). Virus removal may be influenced by many factors such as raw material, specific surface area, element content, surface functional group, pore size distribution and surface charge. Nevertheless, as the capacity of the wood-based PACs varied widely from 0.5 to 4 logs, and a coconut-based PAC removed more virus than some wood-based PACs, the difference in virus removal seems to be due to more than the raw materials. The inherent characteristics of PAC listed in Table 1, i.e. specific surface area, element content and surface functional group, obviously had no relationship with the virus removal ($r^2 < 0.4$); other inherent factors most likely had influence on the adsorptive removal. To investigate the factors affecting the removal, we made a comparison in the following sections among two S-PACs that exhibited the highest virus removal (i.e. wood-1 and wood-2 S-PACs) and 2 S-PACs that had similar particle diameters to the superior S-PACs but exhibited the lowest virus removal (i.e. wood-8 and coconut-2 S-PACs).

3.3. Effect of surface charge of PACs on virus removal

When virus and S-PACs were dispersed in buffered Milli-Q water without Ca^{2+}, both particles were highly negatively charged, and the electrostatic repulsive force between them, measured as electrophoretic mobility, was high (Fig. 3). As the Ca^{2+} concentra-

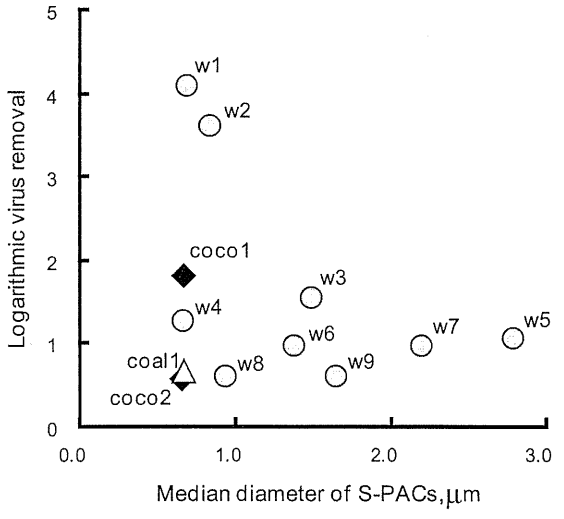

Fig. 2. Relationship between median diameter of S-PACs and virus removal (contact time = 8 h, Ca^{2+} = 100 μM). Circles, diamonds and triangle represent wood-, coconut- and coal-based SPACs. Logarithmic virus removals for wood-1, wood-2, wood-8 and coconut-2 S-PACs were averaged values of two experiments with too small deviations to see, while those for other S-PACs were obtained in one experiment.

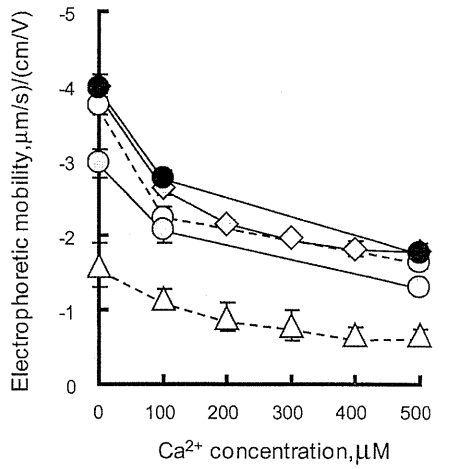

Fig. 3. Electrophoretic mobility of Qβ and S-PACs at different concentrations of Ca^{2+}. White, gray and black circles, gray diamonds and white triangles indicate wood-1, wood-2, wood-8, coconut-2 and Qβ, respectively. Error bars indicate SD of 10 measurements.

tion increased, the electrophoretic mobilities of both virus and S-PACs decreased. In general, an increase in ionic strength compresses the diffuse layer of ions surrounding a charged particle, decreasing the extent of the charge. This behavior has been seen before in viruses [15–18]. Our results support this.

The repulsion energy (V_R) of the electrical double layer between two closely spaced spheres is described as follows [19]:

$$V_R = 2\pi\varepsilon\zeta_1\zeta_2\frac{d_1 d_2}{d_1 + d_2}\exp(-\kappa h) \quad (1)$$

where ε is the permittivity of the medium, ζ_1 and ζ_2 are the zeta potentials of the spheres, d_1 and d_2 are the diameters of the spheres, and h is the minimum surface-to-surface separation between the spheres. κ is the Debye–Hückel reciprocal length:

$$\kappa = \sqrt{\frac{e^2\sum n_{i0}z_i^2}{\varepsilon kT}} \quad (2)$$

where e is the elementary charge, n_0 is the number concentration of ions in the bulk solution, z is the valency of the ion, k is the Boltzmann constant, and T is the absolute temperature. When virus and S-PAC were spaced 0.2 nm apart, as the Ca^{2+} concentration increased, the repulsion decreased (Fig. 4). Virus removal improved from 1–3 logs at 0 μM-Ca^{2+} to 3–6 logs at 500 μM-Ca^{2+}. Thus, virus removal was enhanced as the repulsion decreased. A higher ionic strength compresses the electrical double-layer of charged particles, reducing the electrostatic repulsion between like-charged particles and enabling the particles to move nearer to each other [17,21,22]. The adsorption of the virus onto the S-PAC was most likely hampered by the electrostatic repulsive force between them. Therefore, reducing the repulsion by increasing the ionic strength improved virus removal. One explanation is that the positive ions shield the negative charges on the surfaces of the adsorbate and the adsorbent, decreasing the net electrostatic repulsion between the particles [16,18,20,23]. Or Ca^{2+} may electrically adsorb to a negatively charged moiety of both adsorbate and adsorbent concurrently, forming a cation bridge to link the like-charged particles [18,23,24].

Fig. 5 shows the relationship between the virus removal and the electrical double layer repulsion energy. Virus removal tended to increase as the repulsive force decreased, but the removal performances were different among s-PACs. Wood-1 S-PAC exhibited superior virus removal across all repulsion energy range: the virus removal with wood-1 S-PAC was always greater than those with other S-PACs tested even in the range in which the repulsive force

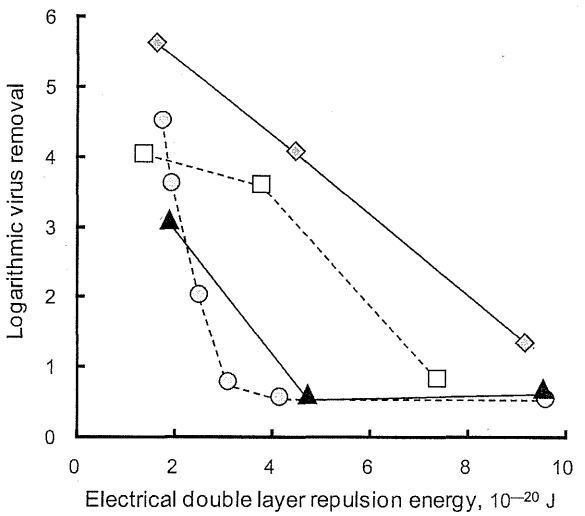

Fig. 5. Relationship between virus removal (Qβ, contact time = 8 h) and repulsion energy of electrical double layer (0.2 nm distance). Gray diamonds, white squares, black triangles and gray circles indicate wood-1, 2, 8 and coconut-2, respectively. Repulsion energy was controlled by Ca^{2+} concentration.

working between the virus and S-PAC particles was the same. These observations mean that the electrostatic repulsion can explain the extent of virus removal by each S-PAC under different ionic conditions, but not the difference between different types of PAC.

The logarithmic virus removals of wood-1 and wood-2 S-PACs linearly increased with decrease in the electrical double layer repulsion energy. In contrast, the virus removals of wood-8 and coconut-2 S-PACs did not change even when the repulsion energy decreased down from 10×10^{-20} to 3×10^{-20} J, but seem to increase drastically when the repulsion energy was smaller than 3×10^{-20} J. Possible reason for this observation is discussed in the following section.

3.4. Effect of pore size distribution of PACs on virus removal

SEM observations revealed that the wood-1 and wood-2 S-PACs, which could remove virus effectively, had a rough surface with many mesopores 20–50 nm in diameter (Photo 1). In contrast,

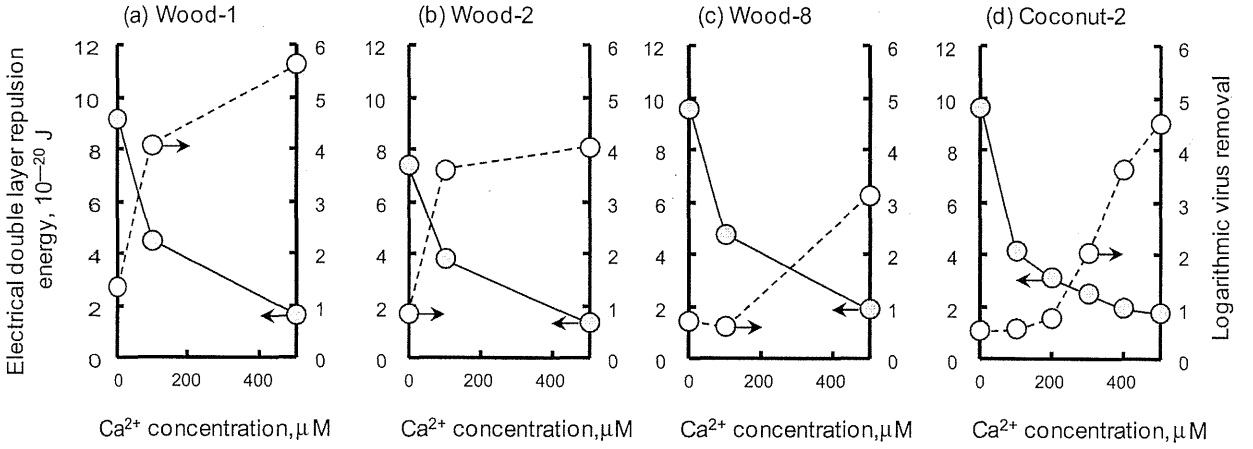

Fig. 4. Changes in repulsion energy of electrical double layer between the virus and S-PACs at 0.2 nm distance, and virus removal (Qβ, contact time = 8 h) with increase in Ca^{2+} concentration. Gray and white circles indicate the electrical double layer repulsion energy and the logarithmic virus removal, respectively.

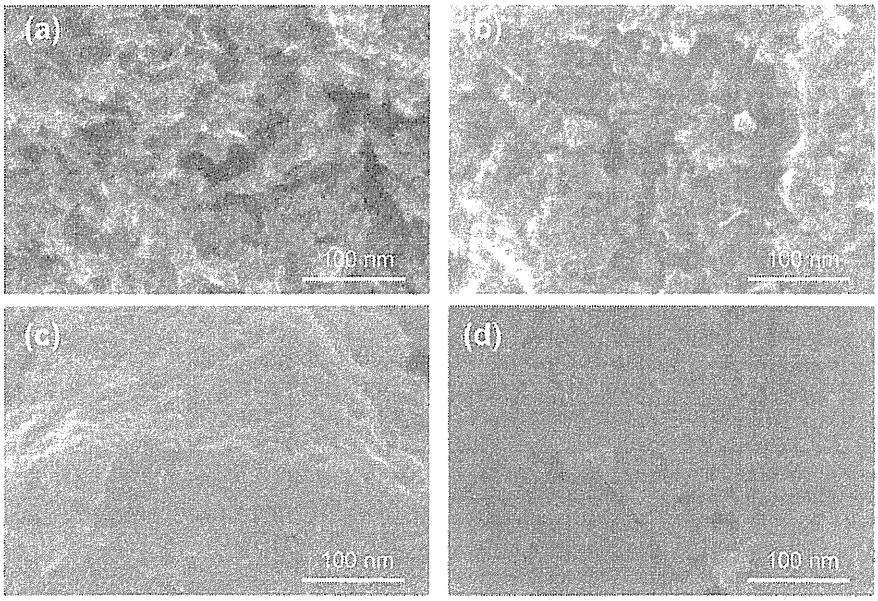

Photo 1. SEM images of S-PAC surfaces: (a) wood-1; (b) wood-2; (c) wood-8; and (d) coconut-2.

Table 2
Comparison in pore volume among S-PACs.

Pore diameter (nm)	Wood-1	Wood-2	Wood-8	Coconut-2
1–2	0.203	0.123	0.206	0.177
2–3	0.040	0.040	0.056	0.030
3–5	0.071	0.091	0.053	0.044
5–10	0.063	0.088	0.038	0.037
10–20	0.044	0.066	0.025	0.028
20–50	0.035	0.039	0.017	0.022

Table 3
Logarithmic removals of Qβ and MS2 with S-PACs (contact time = 8 h, Ca^{2+} = 100 μM).

	Wood-1	Wood-2
Qβ	4.1	3.6
MS2	3.0	2.9

the wood-8 and coconut-2 S-PACs, whose virus removal was poor, had a relatively smooth surface with no mesopores. With a diameter of ~23 nm, the virus cannot pass through pores smaller than this. The nearer the diameter of an adsorbate molecule is to the pore size of an adsorbent, the greater is the attraction [25]. Therefore, the wood-1 and wood-2 S-PACs, with pores 20–50 nm wide, offered good conditions for the virus to settle in, and so removed it effectively. This most likely contributed to the difference of behaviors of viruses in the relationship between the logarithmic virus removal and the electrical double layer repulsion energy indicated in Fig. 5: the wood-1 and wood-2 could easily capture the virus particles with many suitable pores for the virus particles to settle in even under the large repulsion energy that prevented the adsorption of the virus particles to the wood-8 and coconut-2 S-PACs. At this moment, the reason why the virus removals of wood-8 and coconut-2 S-PACs increased drastically with the decrease in the repulsion energy is not clear.

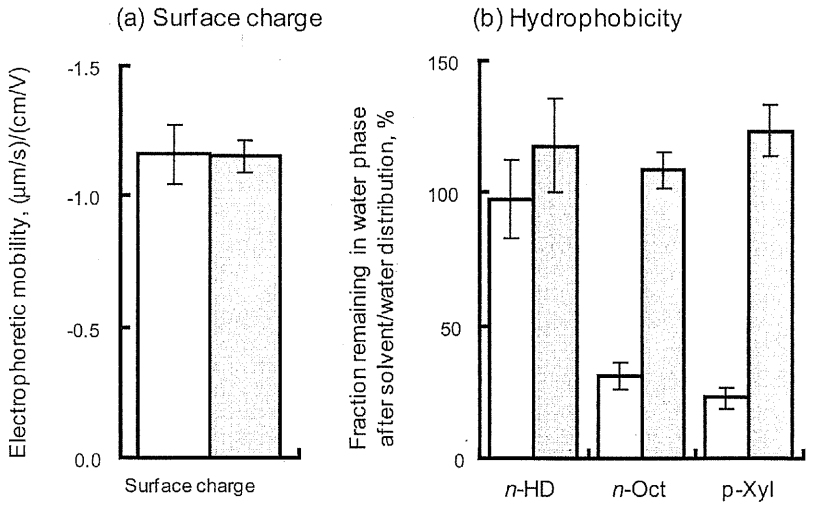

Fig. 6. Comparison of (a) surface charge and (b) hydrophobicity between Qβ and MS2. White and gray columns represent Qβ and MS2, respectively. *n*-HD, *n*-hexadecane; *n*-Oct, *n*-octanol; p-Xyl, p-xylene. Error bars in (a) and (b) indicate SD of 30 and 5 measurements, respectively.

Pore size measurements clearly show that the wood-1 and wood-2 S-PACs had larger pore volume at 20–50 nm than the wood-8 and coconut-2 S-PACs (Table 2); the pore volumes of the high-virus-adsorbable S-PACs were 1.8–2.0 times as much as the averaged pore volume of the low-virus-adsorbable S-PACs. These results agree well with the SEM observations, supporting the hypothesis that the pore size distribution of the S-PACs contributed greatly to virus removal.

3.5. Effect of hydrophobicity of virus on virus removal

The removal of bacteriophage MS2 was ~1 log less than that of Qβ by both wood-1 and wood-2 S-PACs (Table 3). Although the molecular size of an adsorbate controls accessibility to the pores of the activated carbon [26], the diameters of the Qβ and MS2 are almost the same (~23 nm), so this does not explain the difference in removal. Likewise, although the surface charges of viruses depend on the chemistry of their surface proteins, we found no difference in the surface charge between the two viruses (Fig. 6a). Instead, they differed in hydrophobicity (Fig. 6b): MS2 remained in the water phase of all solvent combinations tested, indicating that it has a hydrophilic surface. In contrast, Qβ largely transferred to the solvent phase when *n*-octane and p-xylene were used. This result indicates that the surface of Qβ is more hydrophobic than that of MS2, in agreement with a previous report [27]. Thus, the more hydrophobic the surface of the virus particles is, the greater the virus removal would be expected. As shown in Section 3.3, reducing the surface charge of the activated carbons improved virus removal. The reduction in the surface charge may provide more hydrophobic surface on the carbon apparently, because the reduction allows negatively charged adsorbates to move nearer to the graphite structure on the carbon. Adding to the reduction in the electrophoretic repulsive force, the apparent increase in hydrophobicity of the carbon surface most likely contributed to the high virus removal. Likewise, the hydrophobicity of the viruses contributed to the high removal: the virus having more hydrophobic surface was removed more greatly with the activated carbons.

4. Conclusions

(1) Electrophoretic repulsive force contributed greatly to virus removal: the smaller the repulsion between virus and PAC particles, the greater the virus removal.
(2) The pore size distribution of the PAC contributed greatly to virus removal: PACs with a large volume of pores 20–50 nm in diameter removed virus effectively.
(3) The hydrophobicity of the virus surface contributed greatly to virus removal: the more hydrophobic the surface, the greater the virus removal.
(4) To enhance adsorptive virus removal, activated carbons must have a less negative surface charge and a large volume of pores 20–50 nm wide.

Acknowledgments

Makoto Kobuke and Tomoko Aki made efforts for the experiments on the virus hydrophobicity and the surface functional group of the activated carbons, respectively. This research was supported in part by a Grant-in-Aid for the Encouragement of Young Scientists (2010) from the Ministry of Education, Culture, Sports, Science and Technology of Japan; a Grant-in-Aid (2010) from the Ministry of Health, Labor and Welfare of Japan; and a Kurita Water and Environment Foundation Research Grant (2009).

References

[1] C.P. Gerba, M.D. Sobsey, C. Wallis, J.L. Melnick, Adsorption of poliovirus onto activated carbon in wastewater, Environ. Sci. Technol. 9 (1975) 727–731.
[2] W.A. Hijnen, G.M.H. Suylen, J.A. Bahlman, A. Brouwer-Hanzens, G.J. Medema, GAC adsorption filters as barriers for viruses, bacteria and protozoan (oo)cysts in water treatment, Water Res. 44 (2010) 1224–1234.
[3] P.P. Oza, M. Chaudhuri, Removal of viruses from water by sorption on coal, Water Res. 9 (1973) 707–712.
[4] S.J. Randtke, V.L. Snoeyink, Evaluating GAC adsorptive capacity, J. AWWA 75 (1983) 406–413.
[5] I.N. Najm, V.L. Snoeyink, M.T. Suidan, C.H. Lee, Y. Richard, Effect of particle size and background natural organics on the adsorption efficiency of PAC, J. AWWA 82 (1990) 65–72.
[6] H. Sontheimer, J.C. Crittenden, R.S. Summers, Activated Carbon for Water Treatment, second ed., DVGW-Forschungsstelle, Karlsruhe, Germany, 1988.
[7] Y. Matsui, R. Murase, T. Sanogawa, N. Aoki, S. Mima, T. Inoue, T. Matsushita, Rapid adsorption pretreatment with submicron powdered activated carbon particles before microfiltration, Water Sci. Technol. 51 (6–7) (2005) 249–256.
[8] Y. Matsui, T. Sanogawa, N. Aoki, S. Mima, T. Matsushita, Evaluating submicron-sized activated carbon adsorption for microfiltration pretreatment, Water Sci. Technol.: Water Supply 6 (1) (2006) 149–155.
[9] Y. Matsui, N. Ando, H. Sasaki, T. Matsushita, K. Ohno, Branched pore kinetic model analysis of geosmin adsorption on super-powdered activated carbon, Water Res. 43 (2009) 3095–3103.
[10] N. Shirasaki, T. Matsushita, Y. Matsui, M. Kobuke, K. Ohno, Comparison of removal performance of two surrogates for pathogenic waterborne viruses, bacteriophage Qβ and MS2, in a coagulation–ceramic microfiltration system, J. Membrane Sci. 326 (2009) 564–571.
[11] M.H. Adams, Bacteriophages, Interscience, New York, NY, USA, 1959.
[12] M. Rosenberg, D. Gutnick, E. Rosenberg, Adherence of bacteria to hydrocarbons: a simple method for measuring cell-surface hydrophobicity, FEMS Microbiol. Lett. 9 (1980) 29–33.
[13] N. Shirasaki, T. Matsushita, Y. Matsui, A. Oshiba, K. Ohno, Estimation of norovirus removal performance in a coagulation-rapid sand filtration process by using recombinant norovirus VLPs, Water Res. 44 (2010) 1307–1316.
[14] T. Powell, G.M. Brion, M. Jagtoyen, F. Derbyshire, Investigating the effect of carbon shape on virus adsorption, Environ. Sci. Technol. 34 (2000) 2779–2783.
[15] S.L. Penrod, T.M. Olson, S.B. Grant, Whole particle microelectrophoresis for small viruses, J. Colloid Interface Sci. 173 (1995) 521–523.
[16] J.A. Redman, S.B. Grant, T.M. Olson, J.M. Adkins, J.L. Jackson, M.S. Castillo, W.A. Yanko, Physicochemical mechanisms responsible for the filtration and mobilization of a filamentous bacteriophage in quartz sand, Water Res. 33 (1999) 43–52.
[17] B. Yuan, M. Pham, T.H. Nguyen, Deposition kinetics of bacteriophage MS2 on a silica surface coated with natural organic matter in a radial stagnation point flow cell, Environ. Sci. Technol. 42 (2008) 7628–7633.
[18] S.E. Mylon, C.I. Rinciog, N. Schmidt, L. Gutierrez, G.C.L. Wong, T.H. Nguyen, Influence of salts and natural organic matter on the stability of bacteriophage MS2, Langmuir 26 (2010) 1035–1042.
[19] J. Gregory, Particles in Water: Properties and Processes, CRC Press, Boca Raton, FL, USA, 2006.
[20] J.C. Lance, C.P. Gerba, Effect of ionic composition of suspending solution on virus adsorption by a soil column, Appl. Environ. Microbiol. 47 (1984) 484–488.
[21] D.G. Jewett, T.A. Hilbert, B.E. Logan, R.G. Arnold, R.C. Bales, Bacterial transport in laboratory columns and filters: influence of ionic strength and pH on collision efficiency, Water Res. 29 (1995) 1673–1680.
[22] H. Cao, F.T.C. Tsai, K.A. Rusch, Impact of salinity on MS-2 sorption in saturated sand columns–fate and transport modeling, J. Environ. Eng. 135 (2009) 1041–1050.
[23] J. Zhuang, Y. Jin, Virus retention and transport through Al-oxide coated sand columns: effects of ionic strength and composition, J. Contaminant Hydrol. 60 (2003) 193–209.
[24] M. Pham, E.A. Mintz, T.H. Nguyen, Deposition kinetics of bacteriophage MS2 to natural organic matter: role of divalent cations, J. Colloid Interface Sci. 338 (2009) 1–9.
[25] R.J. Martin, Activated carbon product selection for water and wastewater treatment, Ind. Eng. Chem. Prod. Res. Dev. 19 (1980) 435–441.
[26] C. Moreno-Castilla, Adsorption of organic molecules from aqueous solutions on carbon materials, Carbon 42 (2004) 83–94.
[27] J. Langlet, F. Gaboriaud, J.F.L. Duval, C. Gantzer, Aggregation and surface properties of F-specific RNA phages: implication for membrane filtration processes, Water Res. 42 (2008) 2769–2777.
[28] H.P. Boehm, Some aspects of the surface-chemistry of carbon-blacks and other carbons, Carbon 32 (1994) 759–769.
[29] H.P. Boehm, Surface oxides on carbon and their analysis: a critical assessment, Carbon 40 (2002) 145–149.

WATER RESEARCH 47 (2013) 5819–5827

Available online at www.sciencedirect.com

SciVerse ScienceDirect

journal homepage: www.elsevier.com/locate/watres

Investigating norovirus removal by microfiltration, ultrafiltration, and precoagulation–microfiltration processes using recombinant norovirus virus-like particles and real-time immuno-PCR

Taku Matsushita, Nobutaka Shirasaki, Yuichi Tatsuki, Yoshihiko Matsui*

Graduate School of Engineering, Hokkaido University, N13W8, Sapporo 060-8628, Japan

ARTICLE INFO

Article history:
Received 22 May 2013
Received in revised form
2 July 2013
Accepted 2 July 2013
Available online 12 July 2013

Keywords:
Bacteriophage
Drinking water treatment
MS2
Norovirus
Qβ
Virus-like particles

ABSTRACT

The removal of microorganisms by drinking water treatment processes has been widely investigated in laboratory-scale experiments using artificially propagated microorganisms. However, this approach cannot be applied to norovirus removal, because this virus does not grow in cell or organ culture, and this fact has hampered our ability to investigate its behavior during drinking water treatment. To overcome this difficulty, our research group previously used recombinant norovirus virus-like particles (rNV-VLPs), which consist of an artificially expressed norovirus capsid protein, in laboratory-scale drinking water treatment experiments. However, the enzyme-linked immunosorbent assay (ELISA) method generally used to detect rNV-VLPs is not sensitive enough to evaluate high removal ratios such as those obtained by ultrafiltration (UF). We therefore developed and applied a real-time immuno-polymerase chain reaction (iPCR) assay for rNV-VLP quantification to investigate norovirus removal by microfiltration (MF), UF, and hybrid precoagulation–MF processes. The rNV-VLP detection limit with the developed iPCR assay was improved at least 1000-fold compared with ELISA. Whereas MF with a nominal pore size of 0.1 μm could not eliminate NV-VLPs, a 4-log reduction was achieved by UF with a molecular weight cutoff of 1 kDa. When MF was combined with precoagulation (≥10 μmol-Fe/L for ferric chloride; ≥20 μmol-Al/L for polyaluminum chloride; ≥40 μmol-Al/L for alum), the performance of the hybrid process in eliminating rNV-VLPs was greater than that achieved by the 1 kDa UF. For all processes, the removal ratios of the bacteriophages MS2 and Qβ were greater than the rNV-VLP removal ratios by 1–2 logs, so neither bacteriophage can be recommended as a possible conservative surrogate for predicting the behavior of native NV during these processes.

1. Introduction

Diarrhea is one of the greatest threats to human health worldwide, having been estimated to account for 15% of deaths in children younger than 5 years worldwide in 2008 (Black et al., 2010). Human caliciviruses, including *Norovirus* (NV), are recognized as a leading cause of diarrhea among persons of all ages (Patel et al., 2009). Because NV genome fragments have been detected in environmental waters (Westrell et al., 2006; Aw et al., 2009; Miura et al., 2009),

* *Corresponding author.* Tel./fax: +81 11 706 7279.
E-mail address: taku-m@eng.hokudai.ac.jp (T. Matsushita).
0043-1354/$ – see front matter © 2013 Elsevier Ltd. All rights reserved.
http://dx.doi.org/10.1016/j.watres.2013.07.004

outbreaks of epidemic diarrhea are possible if the raw water to be used for drinking water is contaminated with NV and the water is not adequately treated in the water treatment plant. In fact, Yang et al. (2011) reported that an outbreak of diarrhea due to norovirus in drinking water was caused by raw water contaminated with sewage being inadequately treated for particle removal and virus inactivation in a water treatment plant. Microorganisms can be removed from water by either disinfection or physical separation processes. Accordingly, it is of great importance from the viewpoint of public health to investigate ways to improve the processes used for the removal of NV during water treatment.

Virus-spiking experiments conducted in laboratory-scale treatment plants have been extensively used to investigate virus removal by drinking water treatment processes (Lénès et al., 2010; Bradley et al., 2011; Shi et al., 2012). Before such experiments can be performed, however, the virus must be artificially propagated. As NV does not grow in cell or organ culture and there is no small animal model for NV infection (Hutson et al., 2004), it is impossible to conduct removal experiments by spiking raw water with the artificially propagated virus for treatment by laboratory-scale plants. Accordingly, the removal of NV by drinking water treatment processes has been difficult to evaluate.

To overcome this difficulty, our research group previously investigated NV removal by using an artificially expressed NV capsid protein with a conventional drinking water treatment process consisting of coagulation, sedimentation, and rapid sand filtration (Shirasaki et al., 2010). The NV capsid protein spontaneously self-assembles into virus-like particles (VLPs) when expressed in insect cells infected with a recombinant baculovirus containing the gene encoding the capsid protein (Jiang et al., 1992). Because the recombinant NV VLPs (rNV-VLPs) are morphologically and antigenically the same as native NV particles, rNV-VLPs are expected to behave similarly to native NV during treatment processes. In what to our knowledge was the first attempt to apply rNV-VLPs to evaluate NV removal by drinking water treatment processes, our research group successfully used rNV-VLPs to evaluate NV removal by the conventional drinking water treatment process described above (Shirasaki et al., 2010).

Viruses are continuously and globally monitored in environmental waters. In most cases, the virus concentration is determined either by culturing, where it is reported as the number of plaque-forming units (PFUs), or by polymerase chain reaction (PCR) analysis. Because no culture method has been developed for NV, NV concentrations can be determined only by the latter method. However, rNV-VLPs contain no genomic material, precluding quantification by PCR. In addition to the PCR method, the enzyme-linked immunosorbent assay (ELISA) method has been used for NV quantification; for example, this method has been used with stool samples for the clinical diagnosis of viral infection with good results (Richards et al., 2003). However, ELISA is less sensitive than real-time PCR (Richards et al., 2003; de Bruin et al., 2006). Previously, we used a commercially available ELISA kit for NV to quantify the NV removal performance of the conventional drinking water treatment process (Shirasaki et al., 2010). The quantification was successful because the rNV-VLP concentrations after treatment were relatively high (i.e., the removal ratio was relatively low). However, after filtration through tight membranes with very small pore sizes, smaller rNV-VLP concentrations are expected. The ELISA quantification limit may thus be too poor for this method to be useful for evaluating rNV-VLP concentrations after membrane filtration processes. Thus, this limitation will hamper the use of the ELISA method for the evaluation of NV removal by such processes.

An immuno-PCR (iPCR) assay (Sano et al., 1992) can be used to obtain enhanced sensitivity for the detection and quantification compared with that of the ELISA method. An iPCR assay is an antibody-based immunoassay that uses nucleic acid amplification techniques for signal generation instead of the enzymatic reaction used in the conventional ELISA (Fig. 1). As a result, the sensitivity of the method is dramatically enhanced compared to that of ELISA. The iPCR assay has been applied mainly to the diagnosis of many different kinds of viruses (Maia et al., 1995; Mweene et al., 1996; Constantine et al., 2004; Adler et al., 2005). In the present study, we developed and applied an iPCR assay for the quantification of rNV-VLPs; we then used rNV-VLPs together with the iPCR method to evaluate NV removal by microfiltration (MF), ultrafiltration (UF), and precoagulation–MF processes. This study represents the first time an iPCR assay has been applied to the evaluation of microorganism removal by drinking water treatment processes.

2. Materials and methods

2.1. *rNV-VLP and bacteriophages*

The rNV-VLPs were prepared by a baculovirus–silkworm expression system, as in our previous study (Shirasaki et al., 2010). Briefly, subgenomic cDNA fragments of the NV genome (Chiba virus, AB042808, GI/4, Chiba407/1987/JP) were artificially synthesized. The fragments contained the entire second and third open reading frames and the 3′-UTR (untranslated region) of the NV genome. The cDNA was subcloned into a baculovirus transfer vector, and then the vector was transfected into silkworm cells. The expressed rNV-VLPs were separated from the cell lysate by centrifugation and dialysis. The diameter of the rNV-VLPs was 35.7 ± 3.2 nm (Shirasaki et al., 2010), which roughly corresponds to the particle diameter (approximately 38 nm) previously reported for native NV (Someya et al., 2000). The rNV-VLPs were quantified by an iPCR assay as described in Section 2.2.

Two bacteriophages, Qβ (NBRC 20012) and MS2 (NBRC 102619), were obtained from the National Institute of Technology and Evaluation (NITE) Biological Resource Center (NBRC, Chiba, Japan) for use as model viruses. The diameters of Qβ and MS2 are 23–24 nm (Shirasaki et al., 2009). *Escherichia coli* F^+ (NBRC 13965) obtained from NBRC was propagated for 3 h at 37 °C according to the supplier's instructions to prepare an *E. coli* F^+ suspension. The bacteriophages were then propagated for 22–24 h at 37 °C in the *E. coli* F^+ suspension. The respective bacteriophage cultures were centrifuged (2000 × *g*, 10 min) and then filtered through a membrane filter with a pore size of 0.45 μm (cellulose acetate; DISMIC-25cs; Toyo Roshi Kaisya, Tokyo, Japan). The filtrate was purified by using a centrifugal filter device (molecular weight cutoff [MWCO],

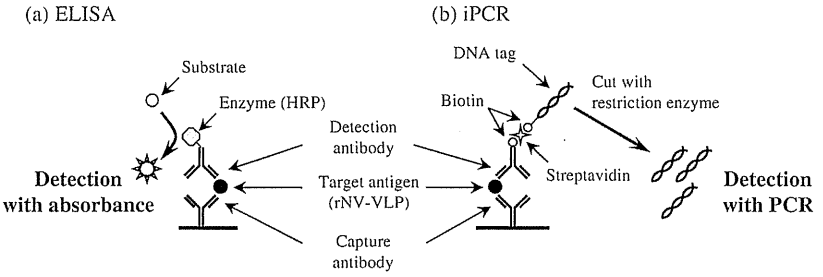

Fig. 1 – Schematic comparison of the ELISA and iPCR methods.

100,000; regenerated cellulose, Amicon Ultra-15; Millipore, Billerica, MA, USA) to prepare the virus stock solution. The bacteriophages were individually quantified by the real-time RT-PCR method with a TaqMan probe and primers (Shirasaki et al., 2009) in an Applied Biosystems 7300 Real-Time PCR System (Applied Biosystems Japan Ltd., Tokyo, Japan).

2.2. *iPCR and ELISA for rNV-VLP quantification*

An iPCR assay was used to quantify the rNV-VLPs. Ten types of monoclonal antibodies to rNV-VLPs were obtained by orally feeding rNV-VLPs to mice (Japan Lamb Ltd., Fukuyama, Japan), and the two most sensitive antibodies out of the 10 antibodies obtained were used for the iPCR assay. One antibody (IgM) was immobilized in the wells of 8-well microplates (TopYield modules, Nalge Nunc International, Penfield, NY, USA) and used to capture the rNV-VLPs, and the other (IgG) was biotinylated and then used for detection. An aliquot of 50 μL of either a sample or a river water (as a negative control) was placed in each well of the 8-well microplates and left at 37 °C for 90 min so as to allow the rNV-VLPs to be captured by the immobilized antibody. The sample solutions were discarded, and then the wells were washed six times with 150 μL of phosphate-buffered saline solution with Tween 20 (PBST). Next, the wells were supplemented with 50 μL of the biotinylated detection antibody (1 μg/mL) in a stabilizing reagent (Immuno Shot Reagent 2, Cosmo Bio Co. Ltd., Tokyo, Japan), and then kept at 37 °C for 90 min so as to allow the detection antibodies to adsorb onto the captured rNV-VLPs. The solutions were discarded, and the wells were washed six times with 150 μL of PBST. The wells were then supplemented with 50 μL of streptavidin (0.1 μg/mL) in a blocking agent solution (1%, Block Ace, DS Pharma Biomedical Co., Ltd., Suita, Japan), and then kept at 37 °C for 60 min so as to allow the avidin to adsorb to the biotin. The solutions were discarded, and the wells were washed six times with 150 μL of PBST. The wells were supplemented with 50 μL of biotinylated DNA tag (480 bp, CareTIS, Co., Ltd., Mobara, Japan), and then kept at 37 °C for 60 min so as to allow the DNA tag to adsorb to the immobilized rNV-VLPs via biotin–avidin interactions. The solutions were discarded, and the wells were washed six times with 150 μL of PBST. The wells were supplemented with 50 μL of EcoRI (restriction enzyme) (Promega KK, Tokyo, Japan) so as to allow a portion of the DNA tag to be released from the immobilized antibody–antigen complex. A portion (4 μL) of the solution was subjected to RT-PCR to measure the rNV-VLP concentration by the SYBR Green method (forward primer, 5′-GAAGGAGCGAGTGACTGAG-3′; reverse primer, 5′-CGTAAT-TACTTAGCCGGTTG-3′) in a Real-Time PCR System following the manufacturer's instructions.

So that we could compare the sensitivity of iPCR for rNV-VLPs with that of ELISA, ELISA was performed with the same two antibodies described above. IgM was immobilized on 8-well microplates to capture the rNV-VLPs, and IgG was conjugated with horseradish peroxidase (HRP) and then used for detection. An aliquot of 50 μL of either a sample or a river water (as a negative control) was placed into each well of the 8-well microplates and left for 90 min at room temperature so as to allow the rNV-VLPs to be captured by the immobilized antibody. The sample solutions were discarded, and the wells were washed six times with 150 μL of PBST. The wells were supplemented with 50 μL of the HRP-conjugated detection antibody (final concentration, 2 μg/mL) in the blocking solution and then kept for 90 min at room temperature so as to allow the detection antibodies to adsorb to the captured rNV-VLPs. The solutions were discarded, and the wells were washed six times with 150 μL of PBST. The wells were supplemented with 50 μL of 3,3′,5,5′-tetramethylbenzidine and kept for 30 min at room temperature to allow the 3,3′,5,5′-tetramethylbenzidine to react with the HRP. After the addition of 50 μL of diluted sulfuric acid (0.3 mol/L) to the wells to terminate the reaction, optical densities at wavelengths of 450 nm and 630 nm in the 8-well microplate were measured with a microplate reader (MTP-300, Corona Electric Co., Ltd., Ibaraki, Japan). Both iPCR and ELISA were performed with two wells for each sample.

2.3. *Membranes*

For UF membranes, we used 47-mm discs made of regenerated cellulose (RC) (Ultracel, Millipore) having different nominal MWCOs of 1, 10, and 100 kDa. Direct filtration experiments with the UF membranes were conducted in a stirred ultrafiltration cell (Model 8050, Millipore) under a constant pressure mode of 500 kPa provided by pressurized nitrogen gas.

We used three types of organic MF membranes and one type of inorganic MF membrane. The organic MF membranes were 45.5-mm discs with a nominal pore size of 0.1 μm composed of polyvinylidene difluoride (PVDF) (hydrophilic Durapore, Millipore), polytetrafluoroethylene (PTFE) (Omnipore, Millipore), or a mixture of cellulose acetate and cellulose

nitrate (MC) (MF-Millipore, Millipore). Direct filtration experiments with an aspirator (EYELA A-1000S, Tokyo Rikakikai Co., LTD., Tokyo, Japan) were performed with the organic MF membranes. The inorganic MF membrane was a monolithic ceramic membrane (55-channel tubular; nominal pore size, 0.1 μm; effective filtration area, 0.043 m^2; membrane diameter, 0.03 m; membrane length, 0.1 m; NGK Insulators, Ltd., Nagoya, Japan), and it was mainly used in the hybrid precoagulation–MF process. The ceramic MF membrane was installed in a stainless steel casing.

2.4. *Direct filtration experiments*

To prepare raw water for the experiments, river water from the Toyohira River (Sapporo, Japan; turbidity, 1.3 NTU; dissolved organic carbon [DOC], 0.6 mg/L; OD_{260}, 0.02 cm^{-1}) was concomitantly spiked with rNV-VLPs (10^{10} VLPs/mL), Qβ (10^8 PFU/mL), and MS2 (10^8 PFU/mL), and the pH of the virus-spiked river water was adjusted to 6.8 with HCl. Fifty milliliters of the raw water was directly filtered using either a stirred ultrafiltration cell or an aspirator. The first 10 mL of the filtrate was discarded, and then the rest was stored for quantification of the rNV-VLPs and the bacteriophages. All direct filtration experiments were conducted three times.

2.5. *Precoagulation–MF experiments*

For the precoagulation–MF experiments, a small inline-coagulation system was used (Fig. 2). The virus-spiked river water was fed into the system at a constant flow rate (58 mL/min) by a peristaltic pump. HCl was added by another peristaltic pump (1 mL/min) before the first in-line static mixer (N40-172, Noritake Co., Ltd., Nagoya, Japan, hydraulic retention time; 1.8 s), with the dose being regulated so as to maintain the pH of the MF permeate at 6.8. When ferric chloride was used as the coagulant, additional experiments were performed at pH 5.8 and 6.3 because the optimum pH for ferric chloride is generally lower than that for aluminum coagulants (Pontius, 1990). Coagulant (polyaluminum chloride [PACl], alum, or ferric chloride) was injected by a peristaltic pump (1 mL/min) after the first in-line static mixer and before the second at various dosing rates (0, 10, 20, or 40 μmol-Al or -Fe/L). After mixing in the second static mixer (hydraulic retention time, 1.8 s), the water was fed into the monolithic ceramic MF module in dead-end mode. The filtration lasted for 30 min without any backwash. Virus concentrations in the raw water tank and in the MF permeate were measured every 5 min. All precoagulation–MF experiments were conducted three times.

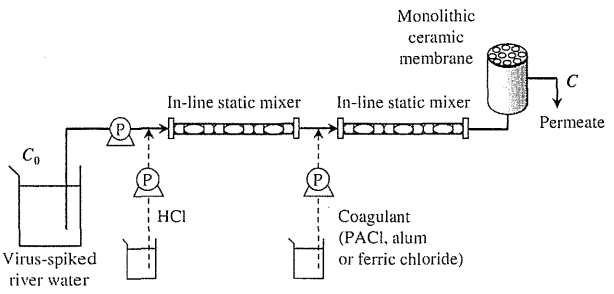

Fig. 2 – Experimental setup of the precoagulation–microfiltration system.

2.6. *Precoated MF experiments*

To investigate whether aluminum flocs retained on the membrane surface affected virus removal, direct filtration experiments were conducted with the ceramic MF membrane precoated with aluminum flocs as follows. Aluminum flocs were accumulated on the membrane surface by continuously feeding unspiked river water (without any virus) into the precoagulation–MF system (PACl, 20 μmol-Al/L). After a predetermined filtration time (30, 60, or 120 min), the raw water was switched to virus-spiked river water, and then direct filtration experiments were conducted on the precoated membranes without any coagulant dosing for the next 30 min. Virus concentrations in the raw water tank and the MF permeate were measured every 5 min.

3. Results and discussion

3.1. *Quantification of rNV-VLPs by the iPCR assay*

We first examined the rNV-VLP calibration curve obtained with the ELISA method (Fig. 3a). The rNV-VLP concentration was linearly correlated with logarithmic absorbance in the range from 10^8 to 10^{10} VLPs/mL, whereas for rNV-VLP concentrations equal to or smaller than 10^8 VLPs/mL, the observed absorbance was constant and almost the same as that of the negative control (Fig. 3a). This results indicates that with the ELISA kit it is possible to quantify rNV-VLP concentrations of $>10^8$ VLPs/mL. This result roughly corresponds to that obtained by using a commercially available ELISA kit for NV (Shirasaki et al., 2010).

The RT-PCR standard curve for the DNA tag used in the iPCR protocol showed a correlation of 1.00 in the range of 10^3 and 10^9 copies/mL (data not shown), indicating that the SYBR Green RT-PCR of the DNA tag was properly conducted. In the iPCR assay developed in the present study, the DNA tag of even the negative control, which contained no rNV-VLPs, was amplified; and a positive threshold cycle (Ct) value was observed (dashed line in Fig. 3b), as has been generally reported by previous studies, probably because of non-specific adsorption of the biotinylated DNA tag (McKie et al., 2002; Adler et al., 2008) or contamination of the reagents or equipment with the DNA tag (McKie et al., 2002). The elevated fluorescence exhibited by the negative control limited the sensitivity of the iPCR assay; but in the range from 10^5 to 10^9 VLPs/mL, the Ct values observed were smaller than that obtained for the negative control. This result means that the iPCR assay could detect rNV-VLPs in that concentration range. In that range, the rNV-VLP concentration was linearly correlated with the Ct value ($r^2 = 0.99$). These results showed that the iPCR method can quantify rNV-VLP concentrations of $\geq 10^5$ VLPs/mL. Thus, the detection limit of the iPCR assay for rNV-VLPs was improved at least 1000-fold compared with that of the ELISA method. Most studies using an iPCR assay have reported a 100- to 1000-fold improvement in the detection

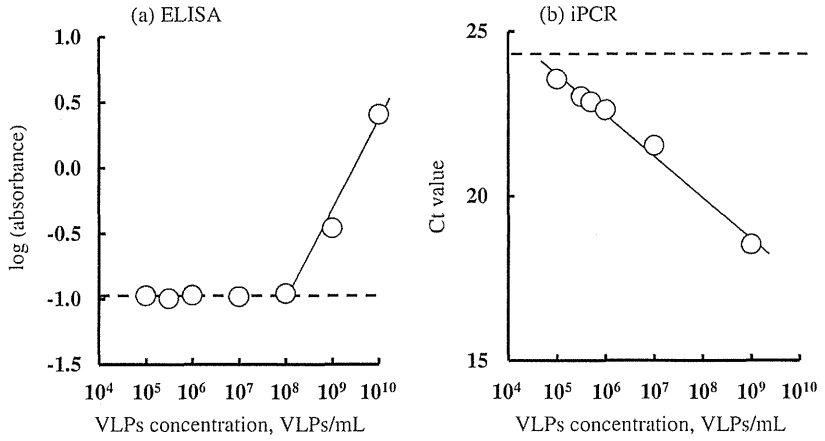

Fig. 3 – rNV-VLP calibration curves obtained with (a) ELISA and (b) iPCR. The dashed lines represent the results obtained with the negative control. Ct value = threshold cycle value.

limit (Adler et al., 2008), in agreement with the result obtained in this study. In our iPCR assay, an aliquot of 50 μL of test sample was added to each well for measurement. Accordingly, the detection limit for rNV-VLPs (10^5 VLPs/mL) is equivalent to 5×10^3 VLPs/well. Tian and Mandrell (2006) developed an iPCR assay for rNV-VLPs and reported a detection limit of 10^2 VLPs/well, which is smaller than our limit, but Adler et al. (2008), who reviewed many iPCR reports, found that the typical detection limit for proteins was approximately 10^3 molecules/well, which is of the same order of magnitude as the detection limit obtained by the present study.

Because the bacteriophages Qβ and MS2 were added to the raw water along with the rNV-VLPs in the membrane filtration experiments conducted in the present study, so that their removal rates could be compared with the rNV-VLP removal rate, the water samples contained not only rNV-VLPs but also the bacteriophages. Accordingly, before performing the membrane filtration experiments, we investigated cross-reactions between the antibodies and the bacteriophages. The river water used in the membrane filtration experiments was first supplemented with both Qβ and MS2 at 10^8 PFU/mL, and then the rNV-VLPs were serially diluted with the bacteriophage-spiked river water to make 10^5–10^9 VLPs/mL of rNV-VLP solution (i.e., the concentrations of the bacteriophages were the same in all diluted rNV-VLP solutions). The iPCR assays performed on the bacteriophage-containing rNV-VLP solutions and on rNV-VLP solutions diluted with river water without bacteriophages revealed no differences between the solutions (data not shown), the indication being that iPCR as employed could quantify rNV-VLPs without cross-reactions occurring, even when the concentration of bacteriophages was high.

3.2. *Removal of rNV-VLPs by the direct MF or UF processes*

We compared virus removal by direct UF or MF (Fig. 4). Irrespective of the composition of the MF membrane, the removal ratios of rNV-VLPs and bacteriophages by the MF membranes were smaller than 0.6 log. Therefore, the MF membranes could not effectively remove viruses from the raw water, because the diameters of the rNV-VLPs and the two bacteriophages (36 and 23–24 nm, respectively) were smaller than the MF membrane pore size (nominally 100 nm). Our results agree with those of a previous study in which the retention of bacteriophage Qβ by MF membranes with a nominal pore size larger than 20 nm was very low (Urase et al., 1996). Herath et al. (1999) also reported that removal ratios of Qβ and MS2 by a MF membrane having a nominal pore size of 50 nm at around pH 7 were 20–30% (i.e., 0.1–0.2 log), values that roughly agree with ours.

The removal ratios of rNV-VLPs were slightly improved with UF membranes having MWCOs of 10 and 100 kDa compared with the MF membranes, but they were still small (approximately 1.5 log). Because an rNV-VLP is composed of 90 capsid protein dimers (Prasad et al., 1994) and each capsid protein has a molecular weight of 58 kDa (Jiang et al., 1992;

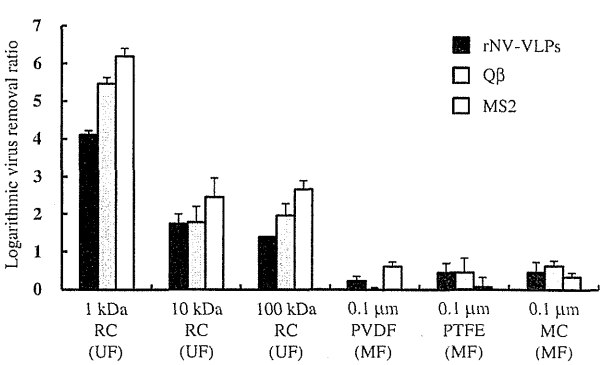

Fig. 4 – Virus removal by different ultrafiltration (UF) or microfiltration (MF) membranes: RC, regenerated cellulose; PVDF, polyvinylidene difluoride; PTFE, polytetrafluoroethylene; MC, mixture of cellulose acetate and cellulose nitrate. The columns and error bars represent the averages and standard deviations, respectively, of three runs.